MSUCL-158
COO-1779-137

THE DECAY OF ^{63}Zn

G. C. Giesler,* Wm. C. McHarris, and R. A. Warner

Department of Chemistry,† Cyclotron Laboratory,‡

and Department of Physics

and

W. H. Kelly

Cyclotron Laboratory‡ and Department of Physics

Michigan State University

East Lansing, Michigan 48824

*Present Address: Los Alamos Scientific Laboratory, Los Alamos, New Mexico 87545.

†Work supported in part by the U.S. Energy Research and Development Administration.

‡Work supported in part by the U.S. National Science Foundation.

Abstract:

Sixty γ rays have been assigned to the decay of 38.0-min ^{63}Zn and have been incorporated into a decay scheme containing 23 levels. In addition to γ-ray singles, anti-Compton, anticoincidence, γ-γ coincidence, and $\gamma^{\pm}$-γ triple coincidence experiments were performed, J^{π} assignments for the nuclear states are based on logft values, relative γ-ray intensities to states of known J^{π}, and charged-particle scattering results. A survey of and comparison with previously reported Ge(Li) detector results and with charged-particle scattering results is presented. The structure of the low-lying states is discussed and compared with calculations and systematics of this region.

[RADIOACTIVITY ^{63}Zn [from ^{63}Cu(p,n)]; measured E_{γ}, I_{γ}, anti-Compton, anticoincidence, γ-γ, $\gamma^{\pm}$-γ, deduced logft, ^{63}Cu deduced levels, J, π. Ge(Li) detector, natural targets.]

1. INTRODUCTION

A primary source of information on nuclear shell structure is the study of nuclides with an unpaired particle or hole and close to a closed shell. One such nuclide is $^{63}_{29}Cu_{34}$, which is one proton and six neutrons above the doubly closed $1f_{7/2}$ shell. Here we have reexamined the decay of ^{63}Zn to ^{63}Cu and have correlated our findings with those of previous investigators and the extensive data from charged particle reactions, inelastic scattering, and numerous theoretical calculations in an attempt to obtain a more coherent understanding of ^{63}Cu states and of nuclear shell structure in this region.

The first report of the production of ^{63}Zn was by Bothe and Gentner[1] in 1937, who produced it by the ^{64}Zn$(\gamma,n)^{63}$Zn reaction, although it appears that Heyn[2] had produced it earlier but did not recognize it mixed in with ^{65}Zn. Since then it has been studied by many groups. Much of the early work[3-7] was devoted to half-life determinations and measuring the β^+ end-point to the ground state of ^{63}Cu. No further reports on the decay of ^{63}Zn appeared until 1947 when Huber et al.[8] reported β^+ feedings to the ground, 0.960-, 1.89-, and 2.60-MeV states with relative intensities of 100:4.5:2:0.2. They also reported α_K for the 960-keV γ transition to be 1.8×10^{-4}. Other groups[9-11] measured cross-sections for producing ^{63}Zn, excitation functions, and its half-life, culminating with the most recent value for its half-life, 38.0±0.1 min, reported by Collé et al.[12]

The first γ-ray studies on ^{63}Zn were reported in 1959 by Hayward et al.[13] and Ricci, Girges, and van Lieshout,[14] with the latter group constructing a decay scheme containing 14 levels. Cumming and Porile[15]

and Vasil'ev, Ch'ang, and Shavtvalov[16] reported more γ-ray studies in 1961 and arrived at decay schemes that more or less confirm that of Ricci, Girges, and van Lieshout. Cumming and Porile also measured the highest β^+ end-point to be 2.33±0.02 MeV and conversion coefficients for the 669-($\alpha_{tot}=5.2\pm0.3\times10^{-4}$) and 961-keV($\alpha_{tot}=2.3\pm0.3\times10^{-4}$) γ's, indicating them both to be $M1$'s.

Of the six reports on γ-ray studies of ^{63}Zn using Ge(Li) detectors, that of Holmberg, Spring, and Lundán[17] was the first and reported 15 transitions in a decay scheme containing 12 levels, in general agreement with the NaI(Tl) studies. De Frenne et al.[18] reported 26 transitions from ^{63}Zn decay, although one of them appears to be the 2615-keV γ from ^{208}Tl (RaC") decay. These were placed in a decay scheme having 22 levels and J^π assignments for 11 of them.

Borchert[19] observed 42 γ rays from ^{63}Zn decay and placed them in a decay scheme having 24 levels with J^π assignments or suggestions for all. He also performed some simple NaI(Tl)-Ge(Li) γ-γ coincidence experiments, and he included a simple discussion of theoretical calculations performed by other groups. His measurement of the relative intensity of the 669-keV γ to the total β^+ feeding is 0.0914±0.0036, which we will discuss later.

The next two papers, those of Kiuru and Holmberg[20] and of Sato and Azuma,[21] are somewhat more conservative. Kiuru and Holmberg placed 31 γ transitions (3 only tentatively) in a decay scheme with 22 levels and J^π assignments for only the lowest 7. Sato and Azuma placed 34 γ transitions in a decay scheme with 21 levels and J^π assignments for 12 of these.

The most recent work, by Klaasse and Gondsmit[22] used Compton suppression and anti-annihilation experiments to reduce the background, performed some Ge(Li)-Ge(Li) γ-γ coincidence experiments, and also relied on our "megachannel" Ge(Li)-Ge(Li) γ-γ coincidence data.[23] They attributed 66 γ rays to ^{63}Zn decay and placed them in a decay scheme having 23 levels, J^{π} assignments or suggestions being made for each.

Meanwhile, since ^{63}Cu, the daughter of ^{63}Zn, is stable as are many of its neighbors, a large variety of charged-particle transfer and inelastic scattering reactions have been performed to study its excited states. Some of these have been ^{63}Cu(p,p'),[24] ^{62}Ni(τ,d),[25] ^{64}Zn(t,α),[26] ^{62}Ni(α,t),[27] and ^{62}Ni(d,n).[28] The in-beam γ-ray reaction, ^{63}Cu$(n,n'\gamma)$,[29] has also been performed, although the results have not yet been published.

Despite all the work that has been performed on ^{63}Zn decay, there remain a number of important discrepancies. Also, still relatively little high-resolution γ-γ coincidence results have been published, and little cross-comparison has been made between the decay-scheme results and the particle-transfer results. Finally, there has been a dearth of trying to understand what the numbers and assignments all mean. We thus try to take an overview in this paper, comparing the various results of the decay-scheme work with the various transfer and scattering reactions and, importantly, with the various kinds of theoretical calculations.

II. SOURCE PREPARATION

The ^{63}Zn sources were prepared by bombarding natural Cu foils (69.09% ^{63}Cu, 30.91% ^{65}Cu) with protons from the Michigan State University Sector-Focused Cyclotron. A 12-MeV beam was used to induce the ^{63}Cu$(p,n)^{63}$Zn reaction. Typically, 0.25-mm thick Cu foils were bombarded for ≈3 min with a beam current of ≈2 μA. The sources were allowed to decay for ≈10 min before being counted for several half-lives. More source was added with the passage of time to maintain a relatively constant counting rate. To insure that only radiations from ^{63}Zn were being observed, the singles γ-ray spectrum was confirmed by counting sources that had been chemically purified by a procedure described elsewhere.[30]

III. EXPERIMENTAL RESULTS

A. γ-Ray Singles Results

Many γ-ray spectra were taken over a long period of time, always using the largest Ge(Li) detectors at our disposal. These included five-sided and true coaxial detectors having efficiencies (compared with a 7.6×7.6-cm NaI(Tl) detector, source distance = 25 cm, E_γ = 1332 keV) of 0.5, 2.0, 2.5, 3.6, 4.6, 10.4, and 18%. The four larger detectors had resolutions of 2.0 keV FWHM at 1332 keV, while the smaller ones were not quite so good. The detector systems used room-temperature FET preamplifiers, low-noise *RC* linear amplifiers having pole-zero compensation, near-Gaussian shaping, and base-line restoration with DC coupling, and 12- and 13-bit ADC's coupled to a PDP-9 or a Sigma-7 computer.

The energies of the prominent γ rays were determined by counting ^{63}Zn sources simultaneously with ^{110m}Ag standards[31] and ^{56}Co standards.[32] The energies of the weaker ^{63}Zn γ rays were then determined by using the energies of the prominent ^{63}Zn γ rays as secondary standards. The centroids and areas of the photopeaks were determined using the computer codes SAMPO[33] and GAMANAL.[34] The intensities were obtained using a previous set of efficiency curves obtained in this laboratory for each detector.[35]

A γ-ray singles spectrum is shown in Fig. 1. Seventy-five γ rays were assigned to ^{63}Zn decay, and their energies and intensities are listed in Table I. (Some of the peaks listed in Table I were obtained with the Compton-and-$\gamma^{\pm}$-suppression system described in the next

section.) There they are compared with the results of the three most extensive previous studies of ^{63}Zn decay. The uncertainties in our energies listed in Table I are based on the uncertainties in the energy standards, the heights of the peaks above the background, and the reproducibility of the calculated energies of the different spectra. The relative intensities listed are averaged from several spectra, and their uncertainties are based on the reproducibilities of the intensities and the uncertainties in our experimentally-determined efficiencies for the detector. They are in general 50% greater than the largest deviation of a value from the average of many runs. The γ-ray intensities of the other authors were renormalized to the 669.68-keV γ while retaining the original number of significant figures. A comparison of our results with the different groups shows reasonable agreement, especially with those of Klaase and Goudsmit,[22] although we observe a number of weaker peaks they could only set upper limits on, and we did not observe a few of their weaker peaks.

Shown in one inset in Fig. 1 is the 1360-1420-keV region of the ^{63}Zn spectrum. Notice here the broadening of the photopeak at ≈1390 keV in comparison to the photopeaks on either side. Because even our best detector could not resolve the 1389.5- and the 1392.3-keV components of the doublet, the program SAMPO was used to strip it, and the results are included in Table I. The other inset shows the two resolved peaks at 1861.1 and 1865.9 keV. These are both photopeaks, neither being the double-escape peak of the 2890.0-keV γ, since both are much stronger than any double-escape peak appearing in the spectrum.

B. Anti-Compton and Anti-$\gamma^{\pm}$ Results

To observe very weak peaks and to lower the background, anti-Compton-anti-$\gamma^{\pm}$ experiments were performed. An 18% efficient Ge(Li) detector having a peak-to-Compton ratio (for the ^{60}Co 1333-keV peak) of ≈38:1 was placed at one end of the tunnel of a 20.3×20.3-cm NaI(Tl) split annulus,[36] which was operated in anticoincidence with the Ge(Li) detector (resolving time, $2\tau \approx 100$ nsec). To depress the 511.01-keV $\gamma^{\pm}$ radiation further, a 7.6×7.6-cm NaI(Tl) detector was placed approximately 1 m from the other (open) end of the annulus tunnel and was also operated in anticoincidence with the Ge(Li) detector. A hot ^{63}Zn source was positioned on a line between the 7.6×7.6-cm NaI(Tl) and the Ge(Li) detectors so that the two detectors presented the same solid angle to the source. With this setup we obtained $\gamma^{\pm}$ reductions as high as a factor of 16, and in Fig. 2 we show a high-statistics spectrum with a reduction of a factor of ≈8. These experiments enabled us to add the weak γ rays to ^{63}Zn decay, and they are included in Table II.

C. Ge(Li)-Ge(Li) Megachannel Coincidence Results

The decay of ^{63}Zn was also examined using a two-dimensional Ge(Li)-Ge(Li) megachannel coincidence system described elsewhere.[37] For this experiment, the 2.5% efficient and 2.0% efficient Ge(Li) detectors were used as the x and y detectors, respectively. The angle between the detectors was ≈150 degrees. In Fig. 3 some of the results are shown, where parts *A* and *E* are the x and y integral or "any" coincidence spectra, respectively. Table III gives the γ-γ coincidence results.

Part *B* shows the results of gating on the 450-keV peak. This gate produces a 962-keV peak greatly enhanced with respect to the 670-keV peak even though the 670-keV peak is stronger in both the singles and integral coincidence spectra. Therefore, the 962-keV γ is clearly in coincidence with the 450-keV γ. Also observed is a peak at 220 keV which results from a Compton scattered γ-ray from one detector being captured in the other. This type of behavior was discussed further for this spectrum in Ref. 37.

The next gate, on the 511-keV region, is shown in part *C*. The γ rays appearing in this spectrum indicate the states that are β^+ fed. Feeding to other states is too weak to be seen in this spectrum. Further results on β^+ feeding to states are given in Section E.

Gating on the 670-keV peak, part *D*, shows only the 511-keV $\gamma^{\pm}$ from the β^+ feeding. Although there is a continuum at energies above 511 keV, no γ transition to the 670-keV level is strong enough to be observed. Part *F* displays the results of gating on the 962-keV peak.

Here the 450-keV γ is greatly enhanced with respect to the 511-keV γ', indicating again the 450-keV γ is in coincidence with the 962-keV γ.

Gating on the 1040-keV γ shows, in part *G*, a spectrum similar to the singles spectrum, but greatly reduced. The appearance of the 1040-keV γ in the singles spectrum is debatable, since it would appear on a Compton edge. It also does not fit anywhere in the decay scheme and is probably a strong background peak that is in chance coincidence with the strong peaks in ^{63}Zn. The gate on the 1392-keV peak, part *H*, shows a coincidence with only one γ ray, the one at 670 keV. This confirms the placement of it as feeding from the 2062-keV level to the 670-keV level. Finally, part *I* shows the results of gating on the 1412-keV peak. Only the 511-keV $\gamma^{\pm}$ from the β^+ feeding appears. No other feeding to this level is strong enough to be seen.

Gating on the remaining peaks in the *x* and *y* integral coincidence spectra show very little if anything. The 1472-keV gates show possible coincidences with 270- and 511-keV γ's. The 1547-keV gate shows only random coincidences and no firm indication of its β^+ feeding. All the counts in this gate were below 550 keV. The other gates are similar in that all the counts appear below 1000 keV. No channel in any of these gates has more than one count in it, and the channels with counts are randomly spaced. The peak at 2754 keV in the integral coincidence spectra could be from ^{24}Na in room background and the Pb collimator.

These data were also analyzed using the digital sum-coincidence technique,[38] where they helped prove the power of that method. The results were completely consistent with those above, so they will not be discussed further here.

D. Anticoincidence Results

To complement the γ-γ coincidence results, anticoincidence experiments were performed using the 20.3×20.3-cm NaI(Tl) split annulus, a 7.6×7.6-cm NaI(Tl) detector, and a 10.4% efficient Ge(Li) detector, with the latter two detectors placed in opposite ends of the annulus tunnel. The γ rays observed by the Ge(Li) detector were counted only when there were no γ rays observed in any of the NaI(Tl) detectors. A description of the system and the electronics is given elsewhere.[36] A spectrum obtained using this system is shown in Fig. 4, and the results are included in Table II. Most of the ground-state transitions observed in this experiment were enhanced over their singles intensities. One of those not enhanced is the 1327-keV γ. This is because the 1327-keV state has no β feeding, and is fed completely by γ transitions from higher-lying states. Other ground-state transitions not enhanced are at 1861, 2012, 2082, and 2093 keV. All these transitions are weak in the singles and were very weak in the anticoincidence results.

E. $\gamma^{\pm}$-γ Triple Coincidence Results

A 511-keV - 511-keV vs. any-γ triple coincidence experiment to determine β^+ feedings was performed using the 20.3×20.3-cm NaI(Tl) split annulus and the 2.5% efficient Ge(Li) detector. The two halves of the annulus were operated separately and each was gated on the 511-keV region. A triple coincidence (resolving time, $2\tau \approx 100$ nsec) was required between the two annulus halves and the Ge(Li) detector. Details of the method are given elsewhere.[36,39,40] A spectrum obtained from this experiment is shown in Fig. 5, and the results are also given in Table II.

The experimental results show β^+ feeding to the 669.68-, 962.16-, 1412.13-, and 1547.1-keV levels. An upper limit of 0.02% has been placed on the β^+ feeding to the 1327.0-keV level. Any β^+ feedings to levels above the 1547.1-keV level were too weak to be observed. A comparison of the measured β^+ feedings to the states and the inferred ε_K/β^+ ratios to the feedings and ratios predicted[41] for allowed transitions is given in Table IV. The experimental values were obtained by calibrating the system using the ^{22}Na 1274-keV peak vs. the 511-keV $\gamma^{\pm}$ in self-gated singles and true $\gamma^{\pm}$-γ coincidence. This leads to good agreement with Borchert's ε_K/β^+ ratio[19] for the 670-keV transition. The differences between the experimental and theoretical values for the first two excited states are small, but they are rather large (even considering the poor statistics) for the other two states. It has recently been discovered,[40] however, that for certain *hindered allowed* transitions the ε/β^+ ratios are quite different from what is

predicted. This can be explained by interferences between second-order and allowed matrix elements in the leptonic part of the current.[41]

IV. DECAY SCHEME

Fig. 6 shows the decay scheme deduced from our experiments with some aid from previous work and the particle-transfer and scattering experiments. Transition and excited-state energies are given in keV, with the adopted energies being a weighted average of our confidence in the various pieces of data. The Q_ε of 3364±8 keV was obtained from ^{63}Cn(p,n) measurements by Birstein et al.[42] and agrees very well with 3.35±0.02 MeV as determined from the β^+ endpoint measured by Cumming and Porile.[15] The (total) transition intensities are given in percent of ^{63}Zn decays. As all the internal conversion coefficients except for the 85.1-keV γ would be less than 0.5% of a given transition intensity, they were ignored. From the measured β^+ feedings and the theoretical ε_K/β^+ ratio[43] for the ground state, the total intensity of the 670-keV γ was calculated. The total feeding intensities for decay to each state were then calculated based on the transition intensities relative to the 670-keV γ. These total feedings are given on the decay scheme to the right of the energy levels, with the exponents in parentheses. Logft values based on them appear in italics at the extreme right of the energy levels. All but the very weakest γ-rays have been placed in this decay scheme. A comparison of these results with those of particle-transfer data is shown in Fig. 7, and a selected, truncated comparison of our results with those of other workers is given in Table V.

V. SPIN AND PARITY ASSIGNMENTS

Inasmuch as a fair amount of confusion exists in the literature, we outline the logic behind our assignments, trying to be as brief as possible.

Ground State

The ground state of stable ^{63}Cu has been assigned $J^\pi=3/2^-$ from the results of many types of particle-transfer experiments, as well as those of other kinds of experiments, including atomic-beams measurements. The logft for β feeding to this state is 5.4, which is consistent with allowed decay from the $3/2^-$ ground state of the ^{63}Zn parent.[44]

669.68-, 962.16-, and 1327.0-keV States

These states have been observed many times in particle-transfer reaction and have been assigned $1/2^-$, $5/2^-$, and $7/2^-$, respectively. The logft's for the first two are well within the range for allowed β decay. No β decay is observed (<0.001%) to the 1327.0-keV state, this in keeping with its being a second-forbidden decay, which would have a logft in the range 10-14 ($\leq 5\times10^{-5}$% feeding). A detailed comparison with results predicted by a number of calculations for these states is given in §VI.

1412.13-keV State

Results from many particle-transfer experiments suggest $5/2^-$ for this state. The logft of 5.8 is consistent with this, as is the γ-deexcitation pattern. Klaasse and Goudsmit[22] (KG) point out a possible difficulty concerning the apparent over-enhancement (a factor of 4.5 to ≈31 over the Weisskopf estimate, depending on what value of Γ_0^2/Γ one uses from resonance-fluorescence measurements[45,46]) of the 742.4-keV ($E2$) γ depopulating this state to the 669.68-keV $1/2^-$ state, and they even use a larger than normal value of r_0 (1.45 fm) to raise the value of the Weisskopf estimate. However, we would like to point out that the internal structure of this state could well be that of the 669.68-keV state (mostly a $p_{1/2}$ single-proton state, cf. §VI) coupled to a 2^+ single-phonon quadrupole vibration, in which case a collectively enhanced $E2$ is not at all unexpected.

1547.1-keV State

β decay to this state has a logft of 6.5, suggesting an allowed or a fast first-forbidden transition. Since the only positive-parity orbital in this shell, $1g_{9/2}$, lies at ≈2510 keV[25] and the first negative-parity core state is a 3^- state at ≈3700 keV in ^{62}Ni, it is expected that positive-parity states should be first observed in ^{63}Cu somewhere above 2 MeV. This state would thus appear to be a negative-parity state fed by an allowed β transition. Although not commonly observed in particle-transfer reactions, ^{64}Zn(τ,α) and ^{63}Cu(d,d') results[47] indicate $J^\pi = 3/2^-$. The γ deexcitation pattern

is consistent with this assignment, and, in fact, the 584.8-keV γ to the 962.16-keV $5/2^-$ state argues against a possible $1/2^-$ assignment.[22]

1861.5-keV State

A J^π of $7/2^-$ was suggested for this state from the ^{64}Zn(^{3}He,α) results[47] because of the large value of the spectroscopic factor (S = 3.3). The logft value of >9 is consistent with this assignment. However, the γ-deexcitation pattern is not. The 1192.4-keV γ populating the $1/2^-$ 669.68-keV state, in fact, rules out $7/2^-$, leaving $5/2^-$ as the most probable assignment. (We were unable to observe the 533.8-keV γ reported by KG, even though we observed other γ rays in this energy range with intensities comparable to what they report for it (0.06±0.02 relative to 100 for the 669.68-keV γ).) KG also present arguments based on unpublished ^{63}Cu(e,e') measurements and on Swann's then preliminary resonance fluoresence results[45] that the 1861.5-keV transition must contain an $M1$ component, thus strengthening the $5/2^-$ assignment. Their argument breaks down, however, for a retarded transition, be it $M1$ or $E2$, and the 1861.5-keV state could well be a complex state with very little similarity to the ground state.

2011.4-keV State

A logft of 7.0 indicates a slow allowed β transition to this state, which decays primarily to the ground state but with a weaker

branch to the $1/2^-$ 669.68-keV state. One could also place the 1048.6-keV γ between this state and the $5/2^-$ 962.16-keV state on the basis of sums. However, both in our work and that of KG, the latter sum is low (KG: 2010.86 vs 2011.32 and 2011.44 keV; this work: 2010.76 vs 2010.88 and 2012.0 keV). Thus, we place this γ-ray only tentatively and make no J^π arguments based on it. Scattering reactions[26] assign $1/2^-$ to the 2011.4-keV state, and the present work is consistent with this assignment, although from the arguments based on Swann's data[45] we retain the $3/2^-$ as a slim possibility.

2062.2-keV State

Various investigators, particle-scattering results included, agree on $1/2^-$ for this state. Our results are also in agreement with this. We do not observe a weak 515.0-keV γ, which KG place between this state and the 1547.1-keV state.

2081.5-keV State

The β feeding to this state has a logft = 6.5. The state in turn decays about 1.5 times as fast to the $7/2^-$ 1327.0-keV state as to the $3/2^-$ ground state. Both the β and γ data thus suggest $5/2^-$ or $3/2^-$. Weak arguments concerning the 754.5-keV γ's having to be a pure (non-enhanced) $E2$ for a $3/2^-$ assignment (also, cf. KG for similar resonance fluorescence arguments) make the $5/2^-$ assignment more likely.

2092.8-keV State

This state receives no observable β feeding. In addition, the ^{64}Zn(t,α) results[26] indicate $J^\pi=7/2^-$. Also, the γ branching from this state to the $5/2^-$ 962.16-keV state is four times that to the $3/2^-$ ground state, which, although a weaker argument, is in agreement with this assignment. We thus choose $7/2^-$, with $5/2^-$ as a less likely possibility.

2336.7-keV State

The logft = 5.7 definitely limits this state to $5/2^-$, $3/2^-$, or $1/2^-$. The γ-deexcitation pattern makes $1/2^-$ unlikely. The ^{64}Zn(t,α) results indicate a $3/2^+$ state, while the ^{62}Ni(τ,d) results indicate it to be $5/2^-$ (they may not be seeing the same state?). Thus, we accept either $5/2^-$ or $3/2^-$ for this state.

2497.6- and 2512.5-keV States

β decay to these states could be either allowed or first-forbidden, telling us only that J^π=1/2, 3/2, or 5/2. We cannot narrow the assignment for the 2512.5-keV state, but Markham and Fulbright[48] deduced $3/2^-$ for the 2497.6-keV state from their ^{65}Cu(p,t) results. KG placed the weak 1169.62-keV γ twice in their decay scheme, depopulating the 2497.6- and/or the 2716.8-keV states. We place it depopulating the 2716.8-keV state.

2535.9-keV State

The $\log ft = 5.3$ for β decay to this state indicates an allowed transition, hence negative parity. The $1/2^-$ possibility is eliminated by the 1208.8-keV γ to the $7/2^-$ 1327.0-keV state. Also, the γ-deexcitation pattern favors $5/2^-$ over $3/2^-$ -- in the absence of collectively enhanced $E2$ transitions, we could eliminate $3/2^-$, but we retain it as a less likely choice.

2697.2-keV State

Again, β decay indicates $1/2^-$, $3/2^-$, or $5/2^-$, and the γ-ray deexcitation pattern is consistent with any of these assignments. The ^{62}Ni(τ,d) reaction,[25] however indicates $1/2^-$.

2716.8-keV State

The β decay to this state is allowed, and the γ-deexcitation pattern eliminates the $1/2^-$ possibility. $5/2^-$ is preferred over $3/2^-$ based on γ-ray intensities, but $3/2^-$ cannot be eliminated given the possibility of enhanced $E2$ transitions.

2780.4-keV State

The β and γ transitions suggest $1/2^-$, $3/2^-$, or $5/2^-$ assignments. This is consistent with the ^{62}Ni(τ,d) results, which indicate $3/2^-$. We do not observe the 244.26-keV γ, which KG place between this state and the 2535.9-keV state.

The Remaining States

From the $\log ft$ values, β decay to the remaining states, at 2807.2, 2858.3, 2889.8, 3045.0, and 3099.9 keV, can be either allowed or first-forbidden, suggesting $1/2^\pm$, $3/2^\pm$, or $5/2^\pm$ assignments for these states. Various particle-transfer reactions popoulate states in this general energy region, but it is difficult to be certain that the states they populate correspond to the states we observe. Assignments for the 2807.2-, 3045.0-, and 3099.9-keV states cannot be narrowed, for each deexcites solely to the ground state. (We do not observe the 1479.08-keV γ that KG place between the 2807.2- and 1327.0- keV states.) The 2858- and 2890-keV states deexcite to $1/2^-$, $3/2^-$, and $5/2^-$ states, allowing us to eliminate the $1/2^+$ and $5/2^+$ possibilities, as $M2$ transitions are not expected here. Also, $3/2^\pm$ is slightly favored in the absence of enhanced $E2$'s, but $1/2^-$ and $5/2^-$ remain less likely choices.

VI. SYSTEMATICS AND DISCUSSION

In addition to the states in ^{63}Cu populated by ^{63}Zn decay, additional states are populated by various scattering and particle-transfer reactions. Fig. 7 shows these up to the ^{63}Zn Q_c. Also, Fig. 8 shows the systematics of the lower-lying states in the odd-mass Cu isotopes.

Many authors have performed calculations on the ^{63}Cu nucleus. The most common approach is using a quadrupole-quadrupole interaction to couple the odd proton to the ground state and the first 2^+ excited state at 1172 keV in ^{62}Ni. Configuration admixing of the $2p_{3/2}$, $2p_{1/2}$, and $1f_{5/2}$ single particle proton states also needs to be included.

Lawson and Uretsky[49] applied the "center of gravity" theorem of atomic j-j coupling to the ^{63}Cu nucleus by assuming that the nucleus was a $2p_{3/2}$ proton coupled to the ^{62}Ni even-even core. The first four excited states of ^{63}Cu were then considered to be the quartet formed by coupling the proton to the 2^+ vibrational first-excited state of ^{62}Ni. By applying this formalism and using the 1412-keV state in ^{63}Cu as the $3/2^-$ member of the quartet, a center of gravity for the 2^+ level was obtained at 1167 keV which compared well with the experimentally determined energy of 1172 keV. Later experiments showed the 1412-keV state to be $5/2^-$ and the necessary $3/2^-$ state has not been found below 2 MeV. No single particle admixtures were used in the calculations.

A "unified" model was used by Bouten and Van Leuven.[50] The ^{62}Ni core was allowed quadrupole surface oscillations with no more than two phonons. The odd proton was in the $2p_{3/2}$, $2p_{1/2}$, or $1f_{5/2}$ orbitals and coupled to surface oscillations. The ground state and first two excited states were used as input parameters to obtain the single-particle level spacings. Good agreement was reached between calculated and experimental values for the electric quadrupole moment and for the $t_{1/2}(E2)$, the transition half-life, for the first two excited states. Although agreement within a factor of two was also reached for the $t_{1/2}(M1)$ for these transitions, poor agreement was reached for the magnetic dipole moment.

Gove[51] applied the calculations of Bayman and Silverberg[52] for coupling a j=3/2 particle to quadrupole surface oscillations to the case of ^{63}Cu. These calculations are in good agreement with the observed $B(E2)$'s. Harvey[53] extended the Bayman-Silverberg model to the magnetic dipole moment and transition probabilities. He obtained good agreement for the dipole moment and for the $B(M1)$ for the transition from the 962-keV state, but his results were a factor of four faster than the $B(M1)$ experimentally obtained for the 670-keV transition.

A strong coupling model was used by Thankappan and True.[54] The even-even ^{62}Ni core which performs quadrupole surface oscillations was coupled by a quadrupole interaction with a dipole element added to the single proton in the $2p_{3/2}$, $2p_{1/2}$, and $1f_{5/2}$ orbitals. Only the 0^+ ground state and 2^+ first excited state of ^{62}Ni were considered in this calculation. Parameters also used were the orbital spacings of Bouten and Van Leuven; however, these were adjusted for better agree-

ment of the calculations with the experimental results. The agreement for the calculated $B(E2)$'s with experimental results is good, but the fits of the $B(M1)$'s vary from good to very bad. Also, the quadrupole moment is in good agreement as is the dipole moment.

Beres[55] used a very different model, namely, he described the core as a quasiboson of angular momentum 2^+ and the odd proton as a quasiproton of spins $1/2^-$, $3/2^-$, and $5/2^-$. The core and the quasiproton were coupled by a quadrupole interaction. The resultant calculated $B(E2)$'s were in general agreement with experimental results. He also calculated the case of two quasineutrons interacting via a quadrupole interaction with the quasiproton. This method gives a large number of low lying levels, and the collective quartet appears very closely spaced at about 2 MeV with the $B(E2)$ values for this quartet in agreement with those of the other method. This method, however, gives much better agreement for the higher lying positive parity states in ^{63}Cu, and good agreement is also obtained between the calculated inelastic α scattering cross sections and those observed experimentally.

The model used by Kisslinger and Kumar[56] is a modified phenomenological vibrational model with its microscopic description in terms of the pairing-plus-quadrupole model. This involves the coupling of the vibrational phonon with a quasiparticle, using a quasirandom phase approximation.

Simons and Sundius[57] used a vibrational core with up to three phonons coupled to a single particle in the $2p_{3/2}$, $2p_{1/2}$, and $1f_{5/2}$ states. They treated the phonon energy as a free parameter and obtained values somewhat greater than those of Bouten and Van Leuven.

They obtained a reasonable fit for the magnetic dipole and electric quadrupole moments, and the fits to the $B(E2)$ and $B(M1)$ for the 670-keV transition are reasonable. However, the $B(M1)$ for the 962-keV transition does not fit well at all.

A semimicroscopic model of coupling the proton to a quadrupole vibrator was used by Paar.[58] The vibrator was allowed up to three phonons and the proton states included the $2p_{3/2}$, $2p_{1/2}$, $1f_{5/2}$, and $1f_{7/2}$ states. The $1f_{7/2}$ was included since experimental results indicate that the $1f_{7/2}$ is not a good closed shell in this case but is partially empty producing a partially filled $2p_{3/2}$ state. Reasonably good fits were obtained for the $B(M1)$ and $B(E2)$ values and for the magnetic dipole and electric quadrupole moments.

Wong[59] performed shell model calculations for ^{63}Cu using a weak coupling model with the $2p_{3/2}$, $2p_{1/2}$, and $1f_{5/2}$ orbitals for the proton. The energy levels produced by the shell-model calculations are in poor agreement with the experimentally determined energy levels. The fits for the $B(M1)$'s and $B(E2)$'s were only fair, although better agreement was reached for the magnetic dipole and electric quadrupole moments.

The intermediate coupling model developed by Thankappan and True was used by Larner[60] to calculate the states in ^{63}Cu. For the calculations, Larner coupled the 0^+ ground state and 2^+ first excited state of ^{62}Ni to the $2p_{3/2}$, $2p_{1/2}$, and $1f_{5/2}$ orbitals with an interaction that contained both dipole and quadrupole terms. For the first case, he used the experimental energy levels and single-particle strengths as input parameters, while the second case used the experi-

mental energy levels and $B(E2)$ values. The results of both cases gave similar good fits to the energy levels, and the first case also gave good fits to the $B(E2)$'s.

Gomez[61] calculated the low-lying levels of odd-mass copper isotopes using a proton coupled to a quadrupole vibrator and the unified model of Bouten and Van Leuven. A fairly good fit was obtained to the various nuclear properties of these isotopes.

An even-even vibrating core, an extra-core proton quasiparticle and an interaction given by a dipole plus a quadrupole term was used by Paradellis and Hontzeas.[62] Agreement with experiment is only fair and they suggest that the omitted $f_{7/2}$ state may be important in such calculations.

DeJager and Boeker[63] compared the particle-core model used by Bouten and Van Leuven, Simons and Sundius, Paar, and Gomez with the particle-phonon model used by Thankappan and True and Larner by redoing those calculations with the same set of experimental data for each model. Their results indicated that the particle-core model gave much better simultaneous fits to excitation energies, spectroscopic factors and electromagnetic properties than the particle-phonon model.

A conventional shell-model calculation similar to that of Wong but restricted to low-seniority configurations was used by Wang, Chiang, Hsieh and Lin[64] to study both even- and odd-mass Cu isotopes. The results produced better agreement with the odd-mass isotopes than with the even, although a fairly good fit was produced for most of the isotopes.

Erokhina, Isakov, and Lemberg[65] used a Wood's Saxon potential and several of the excited states of the core in their calculations and the results fit experimental data reasonably well.

Although most of the calculations agree on single-particle admixtures, they are in disagreement with quantitative energies and transition probabilities. In particular, everyone except Paar[58] assumes that the $1f_{7/2}$ shell is a good closed shell. The experimental results indicate the 1327-keV $7/2^-$ state must have a 6% single particle admixture which would come from the $1f_{7/2}$ closed shell. This agrees with the results of Goode,[66] which indicate that ^{56}Ni is only 94% a doubly closed nucleus.

Acknowledgements

We thank other members of the MSU nuclear chemistry and physics spectroscopy groups, past and present, including Drs. K. L. Kosanke, R. E. Doebler, R. W. Goles, R. R. Todd, L. B. Samuelson, R. B. Firestone, C. Morgan, and D. Beery who were most helpful in data collection and reduction. We thank Drs. G. G. Slaughter, G. L. Morgan, and J. K. Dickens, ORNL, for sharing with us their data prior to publication. We also thank Dr. R. Woods and the staff of the Los Alamos Tandem Van de Graaff Laboratory for their assistance in several irradiations.

References

[1]W. Bothe and W. Gentner, Naturwiss. 25, 191 (1937); Z. Phys. 106, 236 (1937); Z. Phys. 112, 45 (1939).

[2]F. A. Heyn, Nature 138, 723 (1936); Physica 4, 160 (1937).

[3]M. L. Pool, J. M. Cork, and R. L. Thornton, Phys. Rev. 52, 239 (1937).

[4]L. N. Ridenour and W. J. Henderson, Phys. Rev. 52, 889 (1937).

[5]C. V. Strain, Phys. Rev. 54, 1021 (1938).

[6]L. A. Delsasso, L. N. Ridenour, R. Sherr, and M. G. White, Phys. Rev. 55, 113 (1939).

[7]A. A. Townsend, Proc. Roy. Soc. (London) A177, 357 (1941).

[8]O. Huber, H. Medicus, P. Preiswerk, and R. Steffen, Helv. Phys. Acta 20, 495 (1947).

[9]I. L. Preiss and R. W. Fink, Nucl. Phys. 15, 326 (1960).

[10]L. A. Rayburn, Phys. Rev. 122, 168 (1961).

[11]A. Paulson and H. Liskien, Nukleonik 7, 117 (1965).

[12]R. Collé, R. Kishore, and J. B. Cumming, Phys. Rev. C 9, 1819 (1974).

[13]R. W. Hayward, E. Farrelly-Pessoa, D. D. Hoppes, and R. van Lieshout, Nuov. Cim. 11, 153 (1959).

[14]R. A. Ricci, R. K. Girges, and R. van Lieshout, Nuov. Cim. 11, 156 (1959).

[15]J. B. Cumming and N. T. Porile, Phys. Rev. 122, 1267 (1961).

[16]S. S. Vasil'ev, N. H. Ch'ang, and L. Y. Shavtvalov, Zhur. Eksp. i Teor. Fig. 40, 475 (1961).

[17]P. Holmberg, E. Spring, and A. Lundán, Soc. Sci. Fennica, Commentationes Phys.-Math. 32, No. 12 (1966).

[18]D. DeFrenne, M. Dorikens, L. Dorikens-Vanpraet, and J. Demuynck, Nucl. Phys. A103, 203 (1967).

[19]I. Borchert, Z. Phys. 223, 473 (1969).

[20]A. Kiuru and P. Holmberg, Z. Phys. 233, 146 (1970).

[21]Y. Sato and T. Azuma, Report of the Radiation Center of Osaka Prefecture 11, 83 (1970).

[22]A. A. C. Klaasse and P. F. A. Goudsmit, Z. Phys. 266, 75 (1974).

[23]G. C. Giesler, Ph.D. Thesis, Michigan State University, COO-1779-55 (1971).

[24]M. Mazari, W. W. Buechner, and R. P. deFigueiredo, Phys. Rev. 108, 373 (1957).

[25]A. G. Blair, Phys. Lett. 9, 37 (1964); Phys. Rev. 140, B648 (1965).

[26]D. Bachner, R. Bock, H. H. Duhm, R. Santo, and R. Stock, Nucl. Phys. A92, 487 (1967).

[27]P. Roussel, G. Bruge, A. Bussière, H. Faraggi, and J. E. Testoni, Nucl. Phys. A155, 306 (1970).

[28]A. L. Marusek, Ph.D. Thesis, University of Tennessee, 1970, issued as Oak Ridge National Laboratory Report ORNL-TM-2472 (1970), unpublished.

[29]G. G. Slaughter, G. L. Morgan, and J. K. Dickens, Oak Ridge National Laboratory Physics Division Annual Report for 1972, ORNL-4844, p. 56.

[30]G. C. Giesler, Wm. C. McHarris, R. A. Warner, and W. H. Kelly, Phys. Rev. C 7, 620 (1973).

[31]J. H. Hamilton and S. M. Brahmavar, *International Conference on Radioactivity in Nuclear Spectrocopy, Vanderbilt, 11-15 August 1969, Proceedings* (Gordon and Breach, N. Y., 1972), p. 1323; S. M. Brahmavar, J. H. Hamilton, A. V. Ramayya, E. F. Zganjar, and C. E. Bemis, Jr., Nucl. Phys. A125, 217 (1969).

[32]D. C. Camp and G. L. Meredith, Nucl. Phys. A166, 349 (1971).

[33]J. T. Routti and S. G. Prussin, Nucl. Instr. Meth. 72, 125 (1969); J. T. Routti, Lawrence Berkeley Laboratory Report UCRL-19452 (1969).

[34]R. Gunnick and J. B. Niday, Lawrence Berkeley Laboratory Report UCRL-51061 (1972).

[35]For more details about the various procedures used, see, i.a., R. E. Doebler, Wm. C. McHarris, and W. H. Kelly, Phys. Rev. C 2, 2422 (1970).

[36]R. L. Auble, D. B. Beery, G. Berzins, L. M. Beyer, R. C. Etherton, W. H. Kelly, and Wm. C. McHarris, Nucl. Instr. Meth. 51, 61 (1967).

[37]G. C. Giesler, Wm. C. McHarris, R. A. Warner, and W. H. Kelly, Nucl. Instr. Meth. 91, 313 (1971).

[38]G. C. Giesler, K. L. Kosanke, R. A. Warner, Wm. C. McHarris, and W. H. Kelly, Nucl. Instr. Meth. 93, 211 (1971).

[39]R. B. Firestone, Ph.D. Thesis, Michigan State University, COO-1779-112, 1974.

[40]R. B. Firestone, R. A. Warner, Wm. C. McHarris, and W. H. Kelly, Phys. Rev. Lett. 33, 30 (1974).

[41]R. B. Firestone, Wm. C. McHarris, and B. R. Holstein, to be published.

[42]L. Birstein, M. Harchol, A. A. Jaffe, and A. Tsukrovitz, Nucl. Phys. 84, 81 (1966).

[43]P. F. Zweifel, Phys. Rev. 107, 329 (1957).

[44]N. S. Laulainen and M. N. McDermott, Phys. Rev. 177, 1606 (1969).

[45]C. P. Swann, Phys. Rev. C 13, 1104 (1976).

[46]W. J. Alston III, H. H. Wilson, and E. C. Booth, Nucl. Phys. A116, 281 (1968).

[47]M. Barloutaud, J. Gastebois, J. M. Laget, and J. Quidort, Phys. Lett. 19, 306 (1965).

[48]R. G. Markham and H. W. Fulbright, Nucl. Phys. A203, 244 (1973).

[49]R. D. Lawson and J. L. Uretsky, Phys. Rev. 108, 1300 (1957).

[50]M. Bouten and P. Van Leuven, Nucl. Phys. 32, 499 (1962).

[51]H. E. Gove, Phys. Lett. 4, 249 (1963).

[52]B. F. Bayman and L. Silverberg, Nucl. Phys. 16, 625 (1960).

[53]M. Harvey, Nucl. Phys. 48, 578 (1963).

[54]V. K. Thankappan and W. W. True, Phys. Rev. 137, B793 (1965).

[55]W. P. Beres, Nucl. Phys. 75, 255 (1966); Phys. Lett. 16, 65 (1965).

[56]L. S. Kisslinger and K. Kumar, Phys. Rev. Lett. 19, 1239 (1967).

[57]L. Simons and T. Sundius, Soc. Sci. Fennica, Commentationes Phys.-Math. 34, No. 9 (1969).

[58]V. Paar, Nucl. Phys. A147, 369 (1970).

[59]S. S. M. Wong, Nucl. Phys. A159, 235 (1970).

[60]D. Larner, Phys. Rev. C 2, 522 (1970).

[61]J. M. G. Gomez, Nucl. Phys. A173, 537 (1971).

[62]T. Paradellis and S. Hontzeas, Can. J. Phys. 49, 1750 (1971).

[63]J. L. DeJager and E. Boeker, Nucl. Phys. A216, 349 (1973).

[64]M. C. Wang, H. C. Chiang, S. T. Hsieh, and E. K. Lin, Nuov. Cim. 29, 49 (1975).

[65]K. I. Erokhina, V. I. Isakov, and I. Kh. Lemberg, Bull. Acad. Sci. USSR, Phys. Ser. 34, 1914 (1970).

[66]P. Goode, Bull. Am. Phys. Soc. 14, 623 (1969).

[67]H. J. Kim, Nuclear Data Sheets 17, 485 (1976); R. L. Auble, Nuclear Data Sheets 16, 1 (1975), 16, 351 (1975), 16, 417 (1975).

Table I. Energies and Relative γ-Ray Intensities for the Decay of ^{63}Zn

# on Fig. 2	Present Work		Klaasse and Goudsmit (Ref. 22)		Borchert (Ref. 19)		Kiuru and Holmberg (Ref. 20)	
	E	I	E	I	E	I^a	E	I^a
1	85.1 ± 0.5	0.02 ± 0.01	85.00	<0.1	----	----	----	----
	----	----	134.99	<0.01	----	----	----	----
	----	----	219.99	<0.01	----	----	----	----
	----	----	244.26 ± 0.50	0.065 ± 0.010	----	----	----	----
	----	----	292.44	<0.035	----	----	----	----
	----	----	314.23	<0.02	----	----	----	----
	----	----	365.22 ± 0.40	0.14 ± 0.03	364.5 ± 2.0	0.2 ± 0.1	----	----
2	435.6 ± 0.7	0.06 ± 0.04	----	----	----	----	----	----
3	443.0 ± 0.5	0.2 ± 0.1	443.13 ± 0.20	0.20 ± 0.05	----	----	----	----
	----	----	449.22	<0.06	450.0 ± 0.5	3.0 ± 0.5	449.8 ± 1.0	2 ± 1
4	449.97 ± 0.2	2.7 ± 0.2	449.93 ± 0.05	2.88 ± 0.20	----	----	----	----
5	475.5 ± 0.7	0.2 ± 0.1	475.8 ± 0.9	0.07 ± 0.04	----	----	----	----
$\gamma^{\pm}$	511.01	2188	----	----	511.0	2190	511.0 ± 0.02	2060
	----	----	515.0 ± 1.0	0.26 ± 0.10	----	----	----	----
	----	----	533.8 ± 0.6	0.06 ± 0.02	----	----	----	----
6	569.3 ± 0.7	0.06 ± 0.03	----	----	----	----	----	----
7	584.8 ± 0.4	0.38 ± 0.15	584.82 ± 0.15	0.40 ± 0.05	----	----	----	----

Table I - Continued

# on Fig. 2	Present Work		Klaasse and Goudsmit (Ref. 22)		Borchert (Ref. 19)		Kiuru and Holmberg (Ref. 20)	
	E	I	E	I	E	I^a	E	I^a
8	624.1 ± 0.5	0.17 ± 0.04	624.26 ± 0.30	0.17 ± 0.04	----	----	----	----
9	657.0 ± 0.8	0.08 ± 0.04	657.41	<0.06	----	----	----	----
10	669.68 ± 0.1	≡100.	669.62 ± 0.05	≡100	669.6 ± 0.2	≡100 ± 3.9	669.75 ± 0.2	≡100 ± 2
11	674.5 ± 0.5	0.2 ± 0.1	675.03 ± 0.60	0.18 ± 0.04	----	----	----	----
12	685.3 ± 0.5	0.07 ± 0.04	685.6 ± 0.6	0.05 ± 0.02	684.7 ± 1.7	0.45 ± 0.16	----	----
13	742.4 ± 0.4	0.69 ± 0.10	742.25 ± 0.10	0.82 ± 0.10	742.5 ± 0.5	0.86 ± 0.13	742.0 ± 1.0	0.7 ± 0.4
14	754.5 ± 0.5	0.28 ± 0.10	754.81 ± 0.80	0.08 ± 0.03	----	----	----	----
15	758.0 ± 0.8	0.16 ± 0.06	----	----	----	----	----	----
16	765.8 ± 0.3	0.16 ± 0.05	765.7 ± 0.5	0.08 ± 0.03	----	----	----	----
17	876.9 ± 0.5	0.06 ± 0.03	877.2 ± 0.8	0.04 ± 0.02	----	----	----	----
18	899.2 ± 0.5	0.14 ± 0.05	899.02 ± 0.40	0.15 ± 0.03	----	----	----	----
19	924.5 ± 0.5	0.10 ± 0.04	924.30 ± 0.50	0.120 ± 0.024	923.5 ± 1.0	0.25 ± 0.09	----	----
20	962.16 ± 0.1	79.8 ± 3.0	962.06 ± 0.04	78.7 ± 4.0	961.9 ± 0.2	78.8 ± 2.2	962.1 ± 0.2	80 ± 2
21	988.8 ± 0.5	0.05 ± 0.03	989.6 ± 0.7	0.047 ± 0.013	----	----	----	----
22	1048.6 ± 0.5	0.06 ± 0.03	1048.78 ± 0.50	0.054 ± 0.014	----	----	----	----
	----	----	----	----	1087 ± 2	0.32 ± 0.11	----	----

Table I - Continued

# on Fig. 2	Present Work		Klaasse and Goudsmit (Ref. 22)		Borchert (Ref. 19)		Kiuru and Holmberg (Ref. 20)	
	E	I	E	I	E	I^a	E	I^a
23	1123.70 ± 0.2	1.40 ± 0.2	1123.72 ± 0.07	1.35 ± 0.14	1123.7 ± 0.3	1.5 ± 0.3	1123.6 ± 1.0	1.6 ± 0.4
24	1130.5 ± 0.5	0.17 ± 0.04	1130.67 ± 0.25	0.16 ± 0.03	----	----	----	----
25	1140.9 ± 0.5	0.02 ± 0.01	----	----	----	----	----	----
26	1149.58 ± 0.3	0.22 ± 0.04	1149.50 ± 0.16	0.23 ± 0.03	1150 ± 2	0.30 ± 0.05	----	----
27	1169.6 ± 0.5	0.05 ± 0.02	1169.62 ± 0.30	0.094 ± 0.020	1168 ± 3	0.20 ± 0.04	----	----
28	1192.4 ± 0.5	0.05 ± 0.03	1191.63	<0.01	1189 ± 3	0.2 ± 0.1	----	----
29	12 ± 1.0	0.012 ± 0.008	----	----	----	----	----	----
30	1208.8 ± 0.7	0.17 ± 0.04	1208.78 ± 0.30	0.15 ± 0.03	1208 ± 2	0.15 ± 0.04	1209.1 ± 1.0	0.3 ± 0.1
31	1221.3 ± 0.5	0.03 ± 0.02	----	----	----	----	----	----
32	1232.4 ± 0.7	0.06 ± 0.03	1233.7 ± 0.5	0.03 ± 0.01	----	----	----	----
33	1327.0 ± 0.4	0.82 ± 0.05	1327.03 ± 0.08	0.84 ± 0.05	1326.4 ± 0.3	0.98 ± 0.12	1327.1 ± 1.0	0.8 ± 0.2
34	1341.2 ± 0.5	0.07 ± 0.02	1341.7 ± 0.6	0.03 ± 0.01	----	----	1340.0 ± 1.0	0.6 ± 0.2
35	1353.6 ± 0.7	0.015 ± 0.008	----	----	----	----	----	----
36	1374.46 ± 0.3	0.42 ± 0.05	1374.47 ± 0.13	0.42 ± 0.03	1374.3 ± 0.3	0.48 ± 0.09	1374.4 ± 1.0	0.4 ± 0.2
37	1389.5 ± 0.5	0.42 ± 0.07	1389.66 ± 0.08	0.52 ± 0.07	----	----	----	----
38	1392.3 ± 0.4	1.23 ± 0.10	1392.55 ± 0.08	1.18 ± 0.18	1391.5 ± 0.4	1.8 ± 0.1	1392.1 ± 1.0	1.8 ± 0.3
39	1412.07 ± 0.2	9.3 ± 0.4	1412.08 ± 0.05	9.08 ± 0.36	1411.9 ± 0.2	8.8 ± 0.3	1412.1 ± 1.0	9.6 ± 1.0

Table I - Continued

# on Fig. 2	Present Work		Klaasse and Goudsmit (Ref. 22)		Borchert (Ref. 19)		Kiuru and Holmberg (Ref. 20)	
	E	I	E	I	E	I^a	E	I^a
40	1432.1 ± 0.5	0.02 ± 0.01	----	----	----	----	----	----
41	1446.2 ± 0.5	0.013 ± 0.007	1445.8 ± 0.4	0.03 ± 0.01	----	----	----	----
	----	----	1479.08 ± 0.50	0.02 ± 0.01	----	----	----	----
42	1501.0 ± 1.0	0.02 ± 0.015	----	----	----	----	----	----
43	1547.0 ± 0.5	1.49 ± 0.15	1547.04 ± 0.06	1.49 ± 0.06	1546.9 ± 0.2	1.4 ± 0.2	1546.6 ± 1.0	1.8 ± 0.3
44	1559.6 ± 0.5	0.012 ± 0.006	----	----	----	----	----	----
45	1573.6 ± 0.5	0.18 ± 0.06	1573.71 ± 0.20	0.20 ± 0.02	1574.0 ± 2.0	0.14 ± 0.04	1573.3 ± 1.0	0.25 ± 0.1
	----	----	1667.2 ± 0.6	0.017 ± 0.007	----	----	----	----
	----	----	1696.6 ± 1.0	0.024 ± 0.012	----	----	----	----
46	1754.5 ± 0.3	0.050 ± 0.012	1754.89 ± 0.50	0.053 ± 0.012	----	----	----	----
47	1826.0 ± 0.8	0.09 ± 0.04	1827.0 ± 0.5	0.051 ± 0.013	1816.9 ± 1.0	0.030 ± 0.003	1825.6 ± 1.0	<0.09
48	1861.1 ± 0.5	0.18 ± 0.05	1861.34 ± 0.30	0.170 ± 0.024	----	----	1863.4 ± 1.0	0.36 ± 0.21
49	1865.9 ± 0.5	0.24 ± 0.04	1866.08 ± 0.30	0.240 ± 0.026	1865.3 ± 0.3	0.38 ± 0.03	----	----
50	1927.1 ± 0.8	0.07 ± 0.02	1927.18 ± 0.70	0.070 ± 0.014	1926.4 ± 2.0	0.07 ± 0.01	----	----
51	1949.3 ± 1.0	0.012 ± 0.007	----	----	----	----	----	----
52	2012.0 ± 0.4	0.13 ± 0.03	2011.44 ± 0.50	0.13 ± 0.02	2012.0 ± 0.5	0.12 ± 0.02	2010.9 ± 1.0	0.15 ± 0.05

Table I - Continued

# on Fig. 2	Present Work		Klaasse and Goudsmit (Ref. 22)		Borchert (Ref. 19)		Kiuru and Holmberg (Ref. 20)	
	E	*I*	*E*	*I*	*E*	*I*[a]	*E*	*I*[a]
53	2026.94 ± 0.3	0.78 ± 0.05	2026.81 ± 0.30	0.68 ± 0.07	2027.2 ± 0.5	0.66 ± 0.11	2026.7 ± 1.0	0.8 ± 0.2
54	2047.0 ± 0.6	0.045 ± 0.010	2046.44 ± 0.80	0.045 ± 0.013	2048.6 ± 1.5	0.08 ± 0.01	----	----
55	2054.0 ± 0.5	0.006 ± 0.003	----	----	----	----	----	----
56	2062.3 ± 0.4	0.39 ± 0.05	2062.11 ± 0.30	0.42 ± 0.04	2062.0 ± 0.8	0.35 ± 0.08	2062.7 ± 1.0	0.4 ± 0.4
57	2081.5 ± 0.6	0.19 ± 0.05	2081.44 ± 0.30	0.18 ± 0.02	2082.0 ± 0.5	0.16 ± 0.04	2082.1 ± 1.0	0.2 ± 0.1
58	2092.5 ± 0.6	0.04 ± 0.02	2092.64 ± 0.50	0.03 ± 0.01	----	----	----	----
59	2103.3 ± 0.6	0.07 ± 0.04	----	----	2103.2 ± 3.0	0.03 ± 0.02	----	----
60	2110.6 ± 0.5	0.09 ± 0.03	2110.76 ± 0.50	0.075 ± 0.015	----	----	----	----
	----	----	2181.8 ± 0.7	0.016 ± 0.010	----	----	----	----
61	2186.6 ± 1.0	0.02 ± 0.01	2188.0 ± 0.7	0.02 ± 0.01	----	----	----	----
62	2220.1 ± 0.7	0.010 ± 0.005	2219.91 ± 0.70	0.036 ± 0.010	----	----	----	----
63	2297.3 ± 0.7	0.017 ± 0.005	----	----	----	----	----	----
64	2336.72 ± 0.3	1.01 ± 0.08	2336.54 ± 0.30	0.91 ± 0.06	2336.5 ± 0.2	1.0 ± 0.07	2336.7 ± 1.0	0.9 ± 0.2
65	2497.6 ± 0.4	0.24 ± 0.03	2497.43 ± 0.40	0.26 ± 0.03	2497.7 ± 0.4	0.25 ± 0.02	2497.1 ± 1.0	0.3 ± 0.2
66	2512.46 ± 0.4	0.11 ± 0.02	2511.97 ± 0.50	0.12 ± 0.02	2512.0 ± 0.5	0.14 ± 0.02	2512.1 ± 1.0	0.09 ± 0.05
67	2536.21 ± 0.3	0.81 ± 0.04	2536.02 ± 0.30	0.81 ± 0.08	2535.9 ± 0.2	0.84 ± 0.04	2536.2 ± 1.0	0.9 ± 0.2
68	2697.90 ± 0.3	0.50 ± 0.04	2696.57 ± 0.30	0.49 ± 0.05	2696.7 ± 0.2	0.47 ± 0.09	2696.7 ± 1.0	0.5 ± 0.2

Table I - Continued

# on Fig. 2	Present Work		Klaasse and Goudsmit (Ref. 22)		Borchert (Ref. 19)		Kiuru and Holmberg (Ref. 20)	
	E	I	E	I	E	I^a	E	I^a
69	2717.3 ± 0.4	0.14 ± 0.01	2716.89 ± 0.40	0.16 ± 0.02	2717.0 ± 0.5	0.13 ± 0.02	2716.8 ± 1.0	0.16 ± 0.05
70	2780.6 ± 0.4	0.17 ± 0.02	2780.29 ± 0.40	0.19 ± 0.02	2780.1 ± 2.0	0.20 ± 0.02	2780.1 ± 1.0	0.19 ± 0.05
71	2807.2 ± 0.5	0.043 ± 0.007	2806.62 ± 0.60	0.05 ± 0.01	2806.5 ± 0.4	0.030 ± 0.007	2807 ± 2	0.05 ± 0.02
72	2858.2 ± 0.7	0.036 ± 0.006	2857.56 ± 0.80	0.04 ± 0.01	2857.4 ± 1.0	0.036 ± 0.008	2856 ± 2	0.04 ± 0.02
	----	----	----	----	2882.1 ± 2.0	0.011 ± 0.003	----	----
73	2890.0 ± 0.6	0.023 ± 0.004	2889.44 ± 0.80	0.03 ± 0.01	2891.1 ± 1.5	0.026 ± 0.005	2890 ± 2	0.03 ± 0.01
74	3045.0 ± 0.8	0.05 ± 0.01	3044.56 ± 0.80	0.06 ± 0.01	3044.9 ± 1.0	0.055 ± 0.011	3044 ± 2	0.06 ± 0.01
	----	----	----	----	3090.8 ± 2.0	0.004 ± 0.002	----	----
75	3099.9 ± 1.0	0.008 ± 0.004	3100.65 ± 0.80	0.007 ± 0.002	3100.9 ± 0.7	0.009 ± 0.002	3101 ± 2	0.02 ± 0.01

[a] Intensities renormalized relative to the 699.71-keV γ retaining the original number of significant figures.

Table II. Intensities of ^{63}Zn γ Rays in Coincidence Experiments

Relative Intensities				
E_γ(keV)	Singles	Anti-Compton	Anticoincidence	$\gamma^{\pm}$-γ
85.1	----	0.024	----	----
435.6	----	0.058	----	----
443.0	----	0.19	----	----
449.97	2.7	2.7	1.72	----
475.5	----	0.19	----	----
511.01	2188	1216	----	31.3
569.3	----	0.059	----	----
584.8	0.22	0.38	----	----
624.1	0.18	0.17	----	----
657.0	----	0.078	----	----
669.68	≡100	≡100	≡100	≡100
674.5	----	0.19	----	----
685.3	----	0.065	----	----
742.4	0.76	0.69	0.56	----
754.5	0.33	0.28	----	----
758.0	----	0.16	----	----
765.8	----	0.16	----	----
876.9	----	0.060	----	----
899.2	0.16	0.14	----	----
924.5	0.13	0.10	----	----
962.16	79.8	78.7	88.4	69.7
988.8	----	0.049	----	----
1021.9	----	0.092	----	----
1048.6	----	0.057	----	----
1123.70	1.3	1.40	1.2	----
1130.5	0.13	0.20	----	----
1140.9	----	0.020	----	----
1149.58	0.21	0.22	0.30	----
1169.6	----	0.053	----	----
1192.4	----	0.051	----	----
1200.2	----	0.012	----	----
1208.8	0.17	0.17	----	----
1221.3	----	0.033	----	----
1232.4	----	0.064	----	----
1327.0	0.84	0.82	0.76	----
1341.2	----	0.068	----	----
1353.6	----	0.015	----	----
1374.46	0.41	0.42	0.44	----
1389.5	0.44	0.42	1.57	----
1392.3	1.24	1.23		----
1412.07	9.3	9.0	12.5	4.5

Table II - Continued

Relative Intensities				
E_γ(keV)	Singles	Anti-Compton	Anticoincidence	$\gamma^{\pm}$-γ
1432.1	----	0.022	----	----
1446.2	----	0.013	----	----
1501.0	----	0.021	----	----
1547.0	1.6	1.5	1.8	0.45
1559.6	----	0.012	----	----
1573.6	0.19	0.18	0.23	----
1754.5	----	0.050	----	----
1826.0	0.11	0.071	0.21	----
1861.1	0.24	0.18	0.22	----
1865.9	0.26	0.24	0.23	----
1927.1	0.082	0.067	0.28	----
1949.3	----	0.012	----	----
2012.0	0.14	0.12	0.14	----
2026.94	0.78	0.63	0.67	----
2047.0	0.041	0.045	0.038	----
2054.0	----	0.006	----	----
2062.3	0.41	0.38	0.81	----
2081.5	0.20	0.17	0.19	----
2092.5	0.057	0.024	0.043	----
2103.3	0.069	0.006	0.062	----
2110.6	0.087	0.061	0.080	----
2186.6	----	0.023	----	----
2220.1	----	0.010	----	----
2297.3	----	0.017	----	----
2336.72	0.99	1.01	1.8	----
2497.6	0.25	0.24	0.46	----
2512.46	0.12	0.11	0.20	----
2536.21	0.80	0.81	1.5	----
2697.90	0.48	0.50	0.87	----
2717.3	0.14	0.14	0.25	----
2780.6	0.18	0.17	0.34	----
2807.2	0.039	0.047	0.091	----
2858.2	0.032	0.039	0.071	----
2890.0	0.026	0.019	0.057	----
3045.0	0.058	0.050	0.098	----
3099.9	0.009	0.007	0.016	----

Table III. ^{63}Zn Megachannel Coincidence Results

Gate Peak (keV)	γ-Rays in Coincidence
449.97	511.01, 669.68, 962.16
511.01	511.01, 669.68, 962.16, 1412.07
669.68	511.01
962.16	449.97, 511.01
1039	511.01, 669.68
1392.3	669.68
1412.07	511.01

Table IV. Comparison of Experimental and Theoretical β^+ Feedings for ^{63}Zn

Level (keV)	β^+ Feeding		ε_K/β^+		Skew Ratio
	Experimental	Theoretical[a]	Experimental	Theoretical[a]	(exp/theor)
670	7.5%	7.3%	0.094	0.13	0.74
962	5.2%	5.2%	0.23	0.23	1.0
1412	0.33%	0.52%	1.9	0.84	2.3
1546	0.032%	0.055%	3.2	1.4	2.3

[a]Ref. 41.

Table V. Comparison of ^{63}Cu States Fed by ^{63}Zn Decay

Present Work		Klaasse and Goudsmit (Ref. 22)		Borchert (Ref. 19)		Kiuru & Holmberg (Ref. 20)	
E	J^π	E	J^π	E	J^π	E	J^π
0	$\frac{3}{2}^-$	0	$\frac{3}{2}^-$	0	$\frac{3}{2}^-$	0	$\frac{3}{2}^-$
669.68	$\frac{1}{2}^-$	669.62	$\frac{1}{2}^-$	669.6	$\frac{1}{2}^-$	669.75	$\frac{1}{2}^-$
962.16	$\frac{5}{2}^-$	962.06	$\frac{5}{2}^-$	961.9	$\frac{5}{2}^-$	962.1	$\frac{5}{2}^-$
1327.0	$\frac{7}{2}^-$	1327.03	$\frac{7}{2}^-$	1326.4	$\frac{7}{2}^-$	1327.1	$\frac{7}{2}^-$
1412.13	$\frac{5}{2}^-$	1412.03	$\frac{5}{2}^-$	1411.9	$\frac{5}{2}^-$	1412.1	$\frac{5}{2}^-$
1547.1	$\frac{3}{2}^-$	1547.02	$\frac{3}{2}^-$	1546.9	$\frac{1}{2}^-,\frac{3}{2}^-$	1546.6	$\frac{1}{2}^-,\frac{3}{2}^-$
1861.5	$\frac{5}{2}^-$	1861.3	$\frac{5}{2}^-,\frac{7}{2}^-$	1865.3	$\frac{5}{2}^-$	1863.4	$\frac{5}{2}^-,\frac{7}{2}^-$
2011.4	$\frac{1}{2}^-(\frac{3}{2}^-)$	2011.1	$\frac{3}{2}^-,(\frac{1}{2}^-)$	2012.0	$\frac{3}{2}^-$	2010.9	---
2062.2	$\frac{1}{2}^-$	2062.2	$\frac{1}{2}^-,(\frac{3}{2}^-)$	2062.0	$\frac{1}{2}^-,\frac{3}{2}^-$	2062.7	---
2081.5	$\frac{5}{2}^-(\frac{3}{2}^-)$	2081.5	$\frac{5}{2}^-(\frac{3}{2}^-)$	2082.0	$\frac{1}{2}^\pm,\frac{3}{2}^\pm,\frac{5}{2}^\pm$	2081.1	---
2092.8	$\frac{7}{2}^-(\frac{5}{2}^-)$	2092.7	$\frac{7}{2}^-$	---	---	---	---
2336.7	$\frac{5}{2}^-,\frac{3}{2}^-$	2336.53	$\frac{3}{2}^-,\frac{5}{2}^-,(\frac{1}{2}^-)$	2336.5	$\frac{5}{2}^-$	2336.7	---
2497.6	$\frac{3}{2}^-$	2496.9	$\frac{3}{2}^-$	2497.7	$\frac{3}{2}^-,\frac{5}{2}^-$	2497.1	---
2512.5	$\frac{1}{2}^\pm,\frac{3}{2}^\pm,\frac{5}{2}^\pm$	2512.0	$\frac{1}{2}^\pm,\frac{3}{2}^\pm,\frac{5}{2}^\pm$	2512.0	$\frac{3}{2}^\pm,\frac{5}{2}^\pm$	2512.1	---
2535.9	$\frac{5}{2}^-,(\frac{3}{2}^-)$	2535.77	$\frac{5}{2}^-,(\frac{3}{2}^-)$	2535.9	$\frac{3}{2}^-,\frac{5}{2}^-$	2536.2	---

Table V - Continued

Present Work		Klaasse and Goudsmit (Ref. 22)		Borchert (Ref. 19)		Kiuru & Holmberg (Ref. 20)	
E	J^π	E	J^π	E	J^π	E	J^π
2697.2	$\frac{1}{2}^-$	2696.5	$\frac{1}{2}^-,\frac{3}{2}^-,\frac{5}{2}^-$	2696.7	$\frac{1}{2}^-,\frac{3}{2}^-$	2696.7	---
2716.8	$\frac{5}{2}^-,(\frac{3}{2}^-)$	2716.70	$\frac{5}{2}^-,(\frac{3}{2}^-)$	2717.0	$\frac{1}{2}^\pm,\frac{3}{2}^\pm,\frac{5}{2}^\pm$	2716.8	---
2780.4	$\frac{3}{2}^-$	2780.4	$\frac{3}{2}^-,\frac{5}{2}^-,(\frac{1}{2}^-)$	2780.1	$\frac{1}{2}^-,\frac{3}{2}^-$	2780.1	---
2807.2	$\frac{1}{2}^\pm,\frac{3}{2}^\pm,\frac{5}{2}^\pm$	2806.4	$\frac{3}{2}^-,\frac{5}{2}^\pm$	2806.5	$\frac{1}{2}^\pm,\frac{3}{2}^\pm,\frac{5}{2}^\pm$	2807	---
2858.3	$\frac{3}{2}^\pm,(\frac{5}{2}^-,\frac{1}{2}^-)$	2857.7	$\frac{1}{2}^\pm,\frac{3}{2}^\pm,\frac{5}{2}^\pm$	2857.4	$\frac{1}{2}^\pm,\frac{3}{2}^\pm,\frac{5}{2}^\pm$	2856	---
				2882.1	$\frac{1}{2}^\pm,\frac{3}{2}^\pm,\frac{5}{2}^\pm$		
2889.8	$\frac{3}{2}^\pm,(\frac{5}{2}^-,\frac{1}{2}^-)$	2889.4	$\frac{1}{2}^\pm,\frac{3}{2}^\pm,\frac{5}{2}^\pm$	2891.1	$\frac{1}{2}^\pm,\frac{3}{2}^\pm,\frac{5}{2}^\pm$	2890	---
3045.0	$\frac{1}{2}^\pm,\frac{3}{2}^\pm,\frac{5}{2}^\pm$	3044.6	$\frac{1}{2}^\pm,\frac{3}{2}^\pm,\frac{5}{2}^\pm$	3044.9	$\frac{5}{2}^-$	3044	---
				3090.8	$\frac{1}{2}^\pm,\frac{3}{2}^\pm,\frac{5}{2}^\pm$		
3099.9	$\frac{1}{2}^\pm,\frac{3}{2}^\pm,\frac{5}{2}^\pm$	3100.7	$\frac{1}{2}^\pm,\frac{3}{2}^\pm,\frac{5}{2}^\pm$	3100.9	$\frac{1}{2}^\pm,\frac{3}{2}^\pm,\frac{5}{2}^\pm$	3101	---

Figure Captions

Fig. 1 ^{63}Zn γ-ray singles spectrum. The inserts show the regions at 1382 keV and 1865 keV in more detail.

Fig. 2 ^{63}Zn γ-ray anti-Compton, anti-$\gamma^{\pm}$ spectrum. The energies corresponding to the numbers are given in Table I.

Fig. 3 ^{63}Zn γ-γ megachannel coincidence spectra. In the top of this Figure and of Part 2 are shown the integral coincidence spectra, and in the lower portions are shown the various selected gates.

Fig. 4 An anticoincidence spectrum from the decay of ^{63}Zn.

Fig. 5 A $\gamma^{\pm}$-γ triple coincidence spectrum obtained using the NaI(Tl) annulus and the 2.5% efficient Ge(Li) detector. The broadening of the 962.16-keV peak resulted from a linear-gate irregularity.

Fig. 6 Proposed decay scheme for ^{63}Zn. For clarity the spin-parity assignments are given as $2J^{\pi}$ (e.g., 3^- means $3/2^-$). All energies are given in keV transition intensities in per cent per ^{63}Zn decay. The three columns at the right list the % ε feeding to a level, the % β^+ feeding, and the logft, respectively.

Fig. 7 A summary of various reactions used to study excited states in ^{63}Cu.

Fig. 8 Systematics of the odd-mass Cu isotopes. The results shown are from Ref. 67 and the present work.

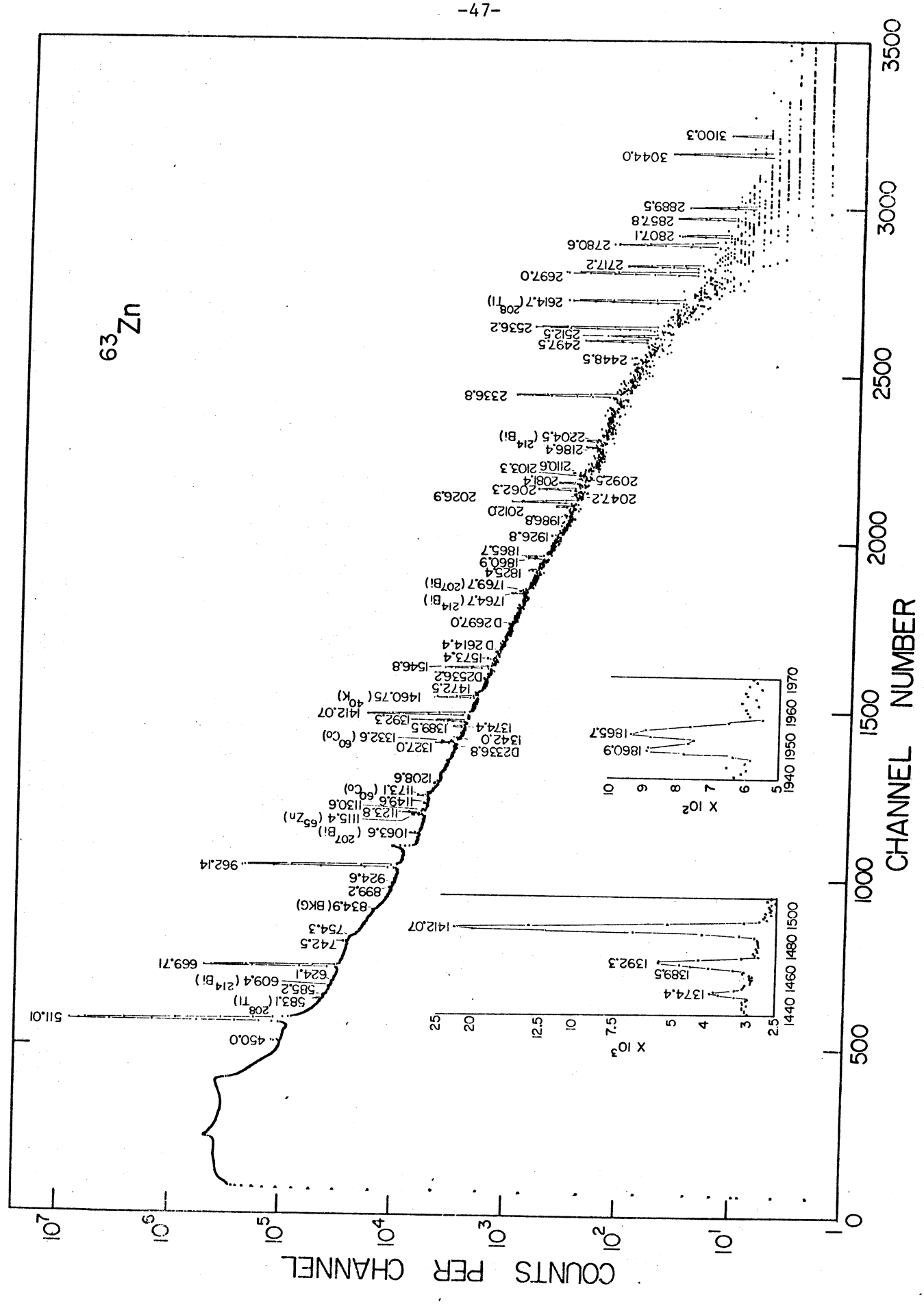
63Zn
COUNTS PER CHANNEL
CHANNEL NUMBER
511.01
450.0
583.1 (208Tl)
585.2
609.4 (214Bi)
624.1
669.71
742.5
754.3
834.9 (BKG)
899.2
924.6
962.14
1063.6 (207Bi)
1115.4 (65Zn)
1123.8
1130.6
1149.6
1173.1 (60Co)
1208.6
1327.0
1332.6 (60Co)
1342.0
1374.4
1389.5
1392.3
1412.07
1460.75 (40K)
1472.5
1546.8
1573.4
1764.7 (214Bi)
1769.7 (207Bi)
1825.4
1860.9
1865.7
1926.8
1986.8
2012.0
2026.9
2047.2
2062.3
2081.4
2092.5
2103.3
2110.6
2186.4
2204.5 (214Bi)
2336.8
2448.5
2497.5
2512.5
2536.2
2614.7 (208Tl)
2697.0
2711.2
2780.6
2807.1
2857.8
2889.5
3044.0
3100.3

Figure 1

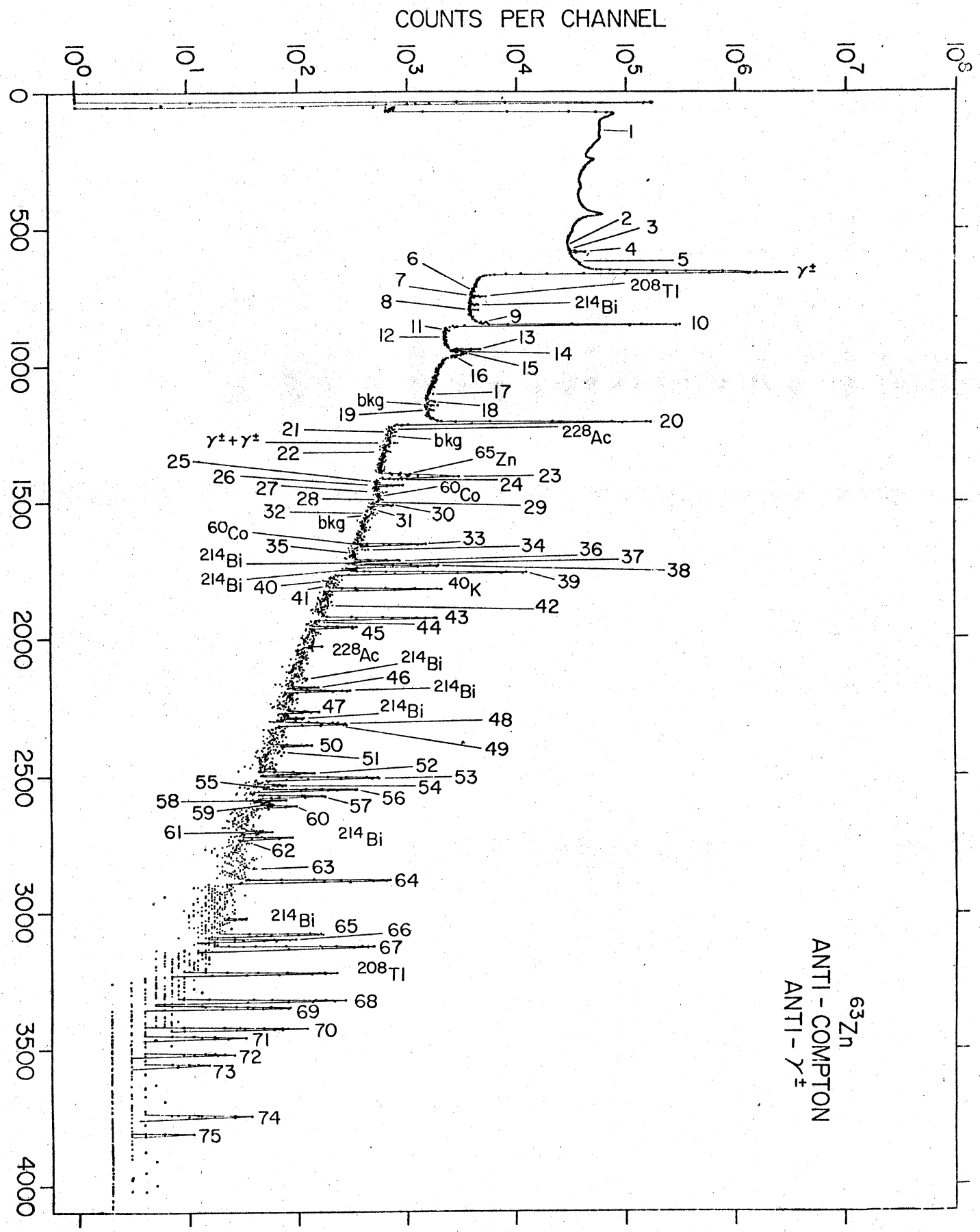
COUNTS PER CHANNEL
10^0
10^1
10^2
10^3
10^4
10^5
10^6
10^7
10^8
CHANNEL NUMBER
0
500
1000
1500
2000
2500
3000
3500
4000
^{63}Zn
ANTI - COMPTON
ANTI - $\gamma^{\pm}$
1
2
3
4
5
$\gamma^{\pm}$
6
7
^{208}Tl
8
^{214}Bi
9
10
12
11
13
14
16
15
17
bkg
19
18
20
^{228}Ac
21
$\gamma^{\pm}+\gamma^{\pm}$
bkg
22
^{65}Zn
25
23
26
24
27
^{60}Co
28
29
32
bkg
31
30
^{60}Co
33
35
34
36
37
^{214}Bi
38
^{214}Bi
40
39
^{40}K
41
42
43
44
45
^{228}Ac
^{214}Bi
46
^{214}Bi
47
^{214}Bi
48
49
50
51
52
53
55
54
58
56
59
57
60
61
^{214}Bi
62
63
64
^{214}Bi
65
66
67
^{208}Tl
68
69
70
71
72
73
74
75

Figure 2

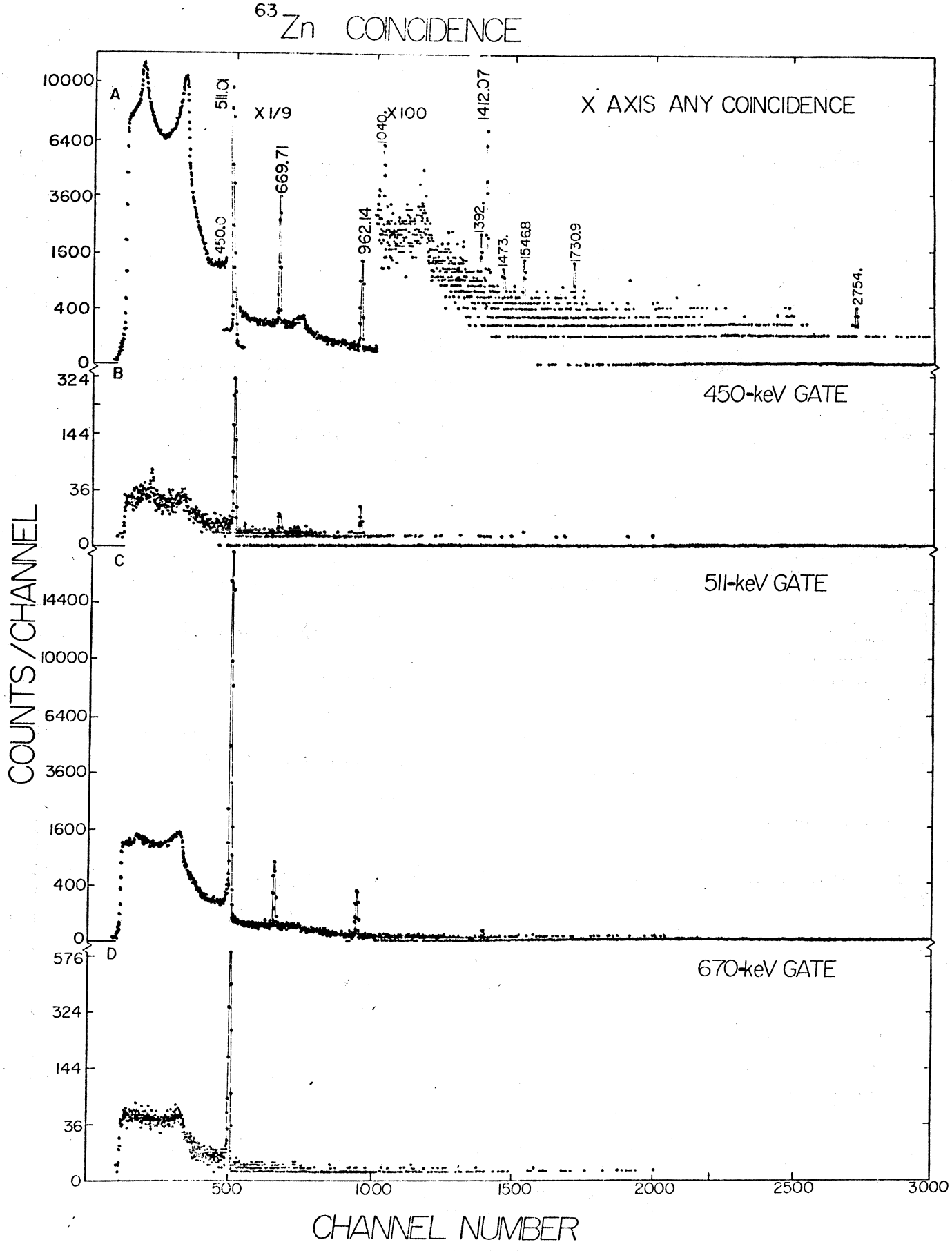
63Zn COINCIDENCE
X AXIS ANY COINCIDENCE
450-keV GATE
511-keV GATE
670-keV GATE
COUNTS/CHANNEL
CHANNEL NUMBER
A
B
C
D
511.0
X 1/9
669.71
450.0
962.14
1040.
X 100
1412.07
1392.
1473.
1546.8
1730.9
2754.
10000
6400
3600
1600
400
0
324
144
36
14400
576
500
1000
1500
2000
2500
3000

Figure 3

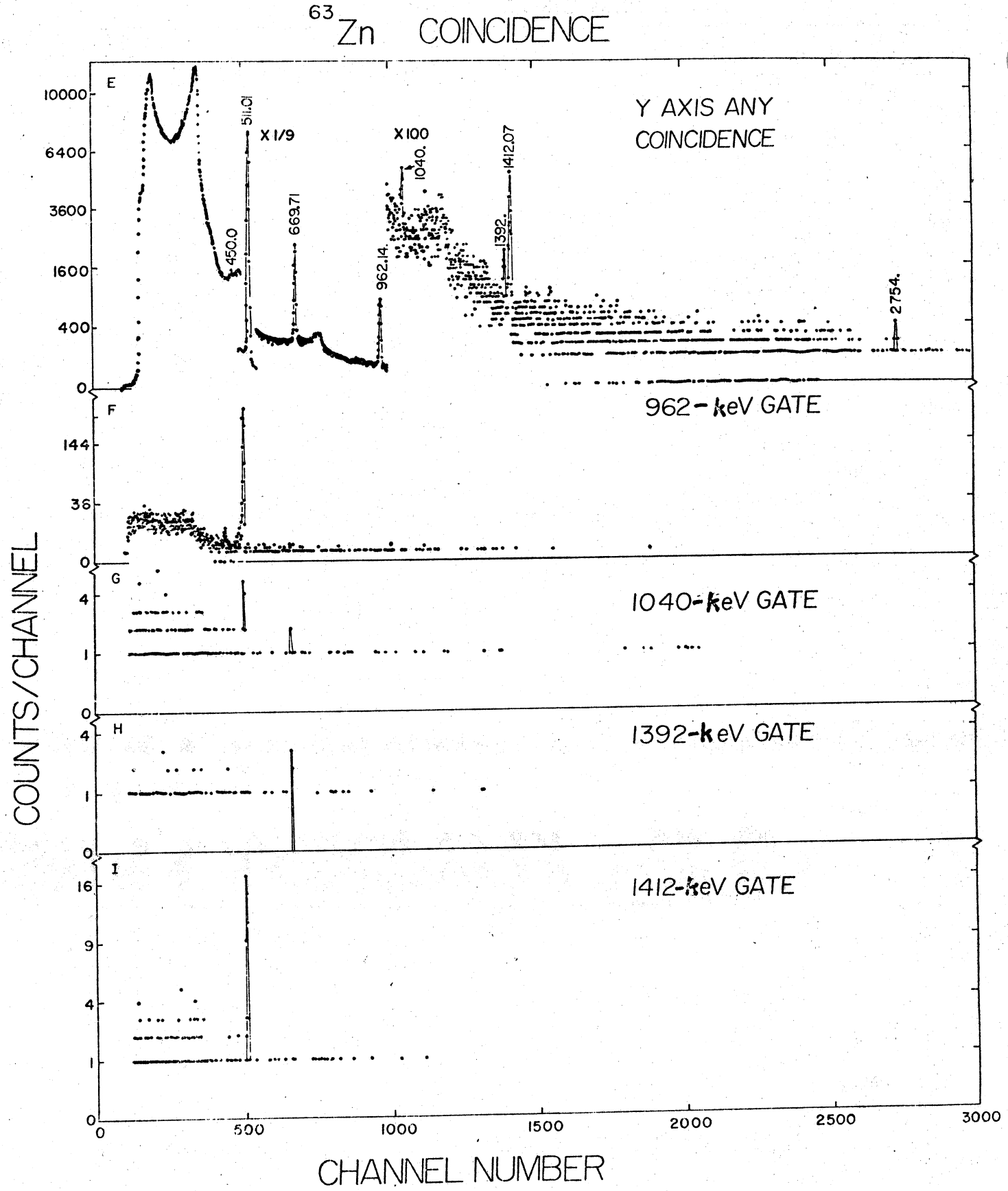
63Zn COINCIDENCE
E
Y AXIS ANY
COINCIDENCE
X 1/9
X 100
511.01
450.0
669.71
962.14
1040.
1392.
1412.07
2754.
F
962-keV GATE
G
1040-keV GATE
H
1392-keV GATE
I
1412-keV GATE
COUNTS/CHANNEL
CHANNEL NUMBER

Figure 3

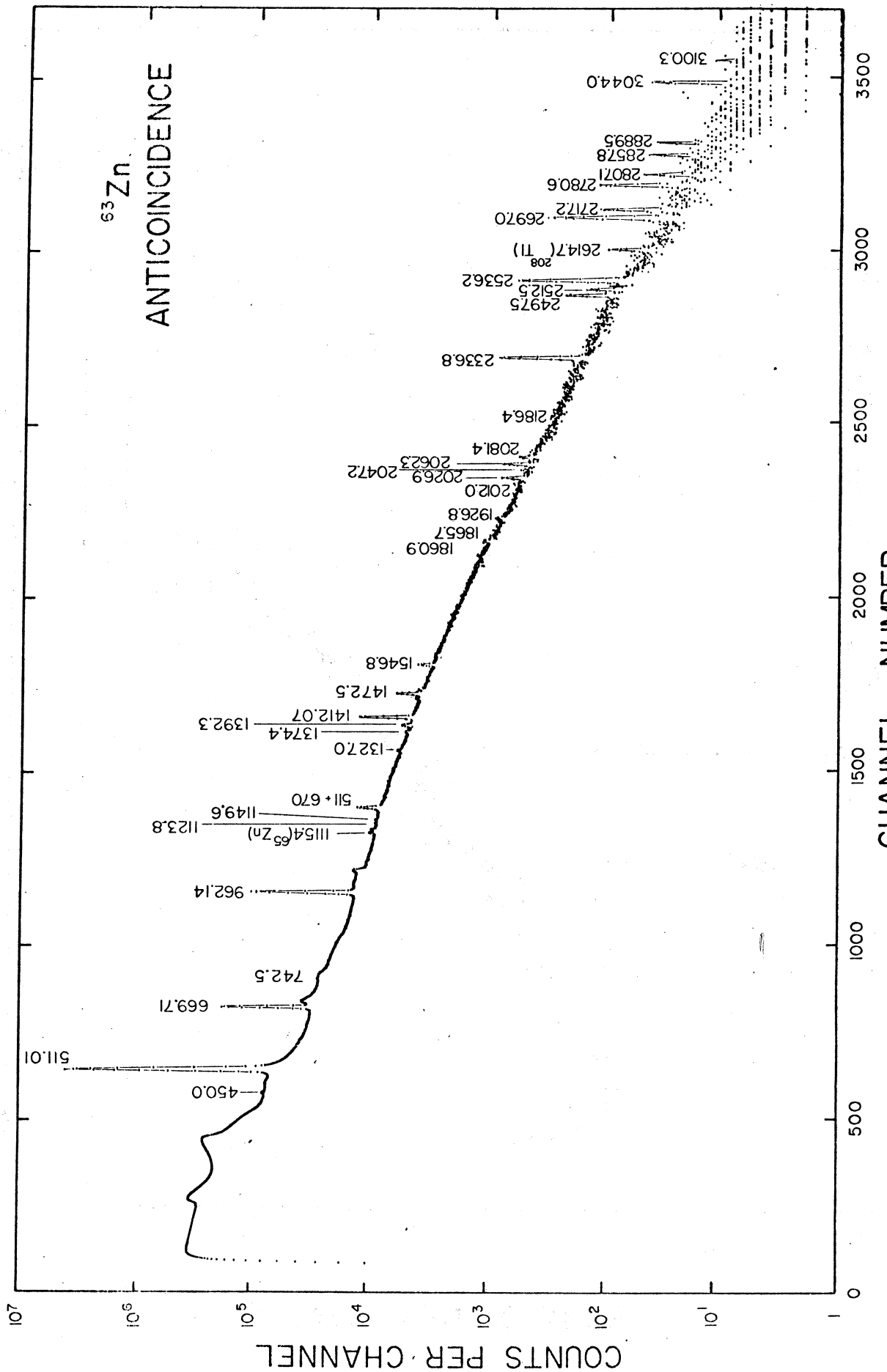
^{63}Zn
ANTICOINCIDENCE
COUNTS PER CHANNEL
CHANNEL NUMBER
511.01
450.0
669.71
742.5
962.14
1115.4(^{65}Zn)
1123.8
1149.6
511 + 670
1327.0
1374.4
1412.07
1392.3
1472.5
1546.8
1860.9
1865.7
1926.8
2012.0
2026.9
2047.2
2062.3
2081.4
2186.4
2336.8
24975
25125
25362
26147(^{208}Tl)
26970
27172
27806
28071
28578
28895
30440
31003

Figure 4

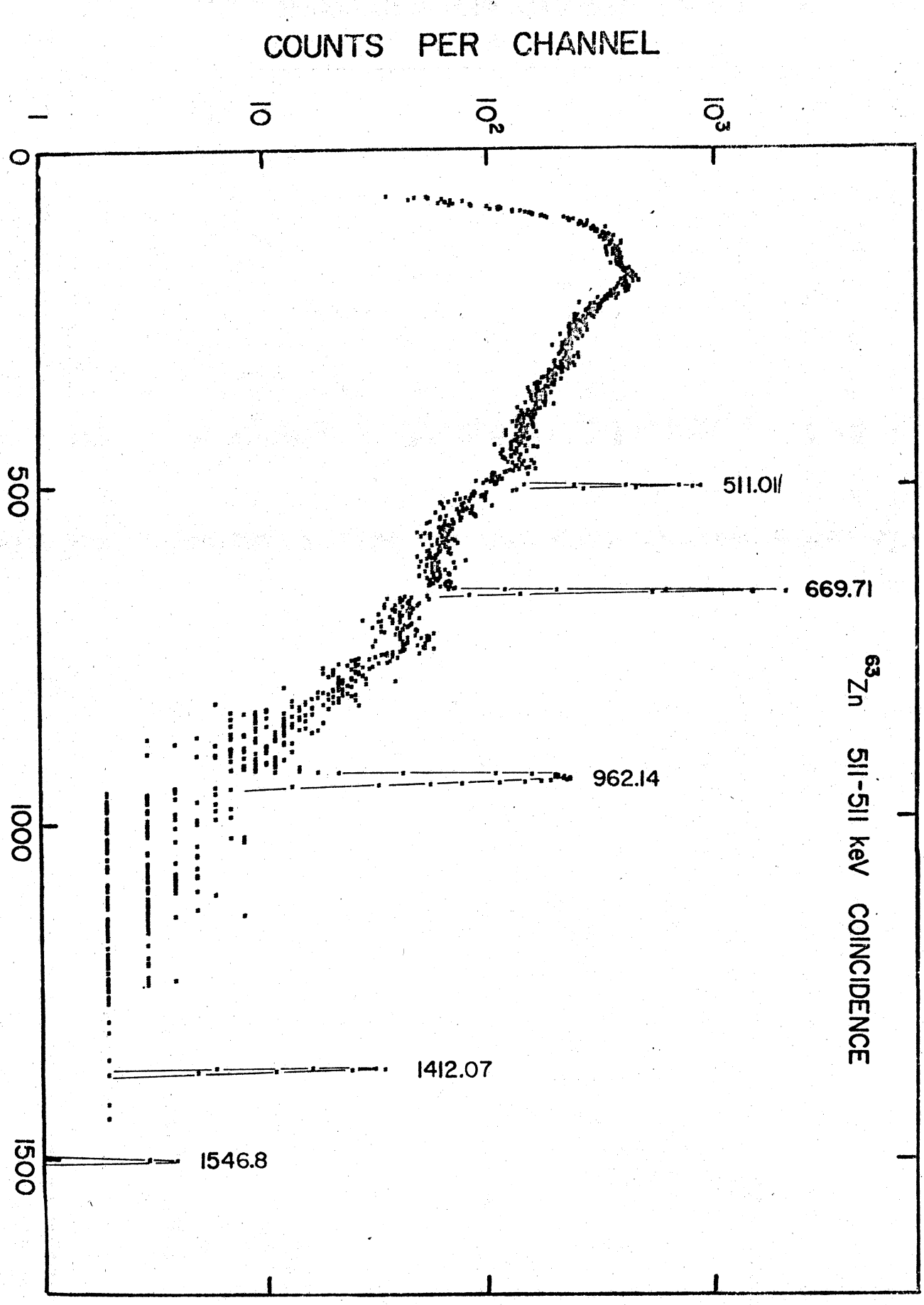
COUNTS PER CHANNEL
10
10²
10³
0
500
1000
1500
511.01
669.71
962.14
1412.07
1546.8
⁶³Zn 511-511 keV COINCIDENCE

Figure 5

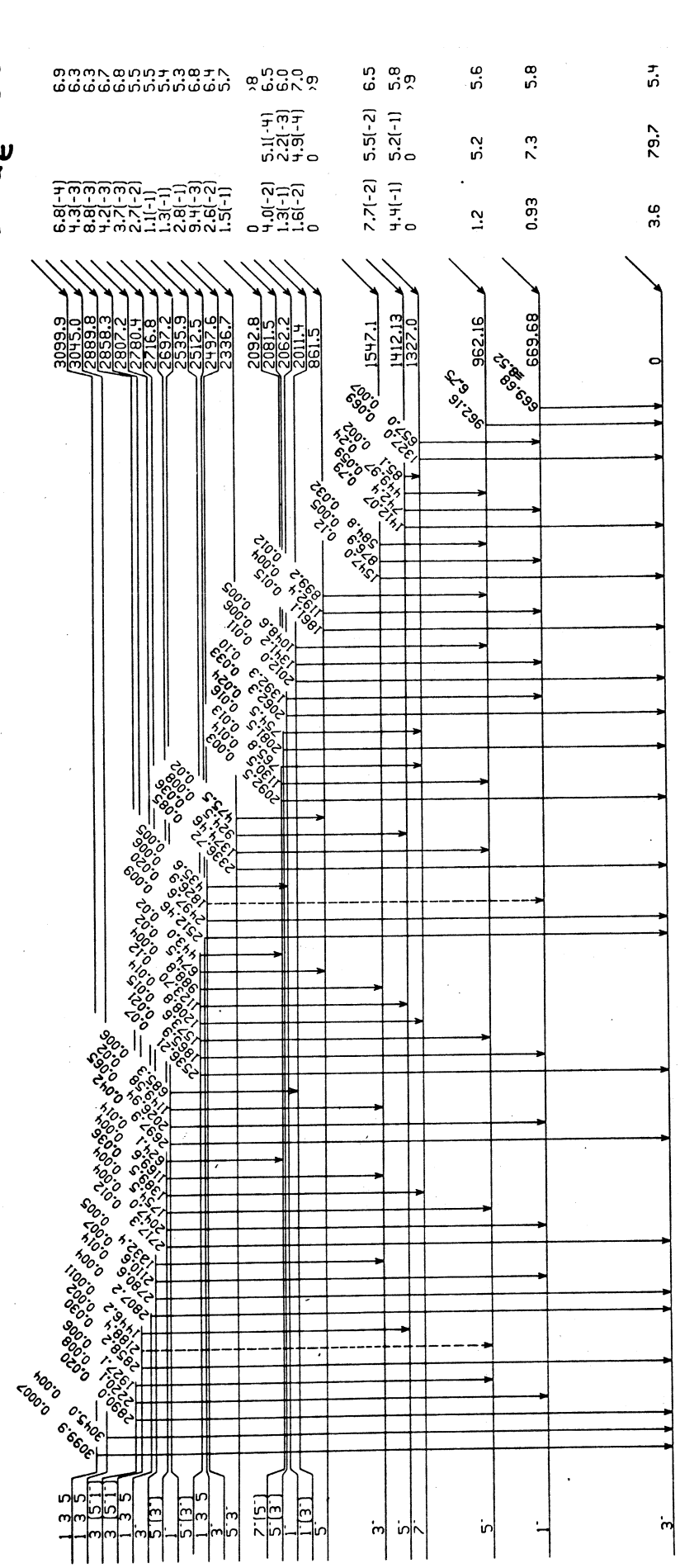

Figure 6


MeV
3
2
1
0
^{63}Zn
1/±,3/±,5/±
1/±,3/±,5/±
3/
3/-
5/-,(3/-)
1/-
5/-(3/-)
1/±,3/±,5/±
3/-
3/-,5/-
7/-(5/-)
5/-(3/-)
1/-(3/-)
1/-
5/-
3/-
5/-
7/-
5/-
1/-
3/-
(5/-,1/-)
1/±,3/±,5/±
1/-
3/-
1/-
9/+
5/-
1/-
5/+
5/-
3/-
5/-
7/-
5/-
1/-
3/-
3/+
7/-
7/-
7/-
9/+
7/-
3/+
7/-
1/-
7/-
3/-
5/-
7/-
5/-
1/-
3/-
9/+
5/-
5/-
1/-
3/-
(3/+,5/+)
1/-,3/-
(7/+,9/+)
1/-,3/-
5/-,7/-
5/-,7/-
5/-
1/-
3/-
^{63}Cu(p,p')
PRESENT WORK
^{62}Ni(τ,d)
^{64}Zn(t,α)
^{62}Ni(α,t)
^{62}Ni(d,n)

Figure 7

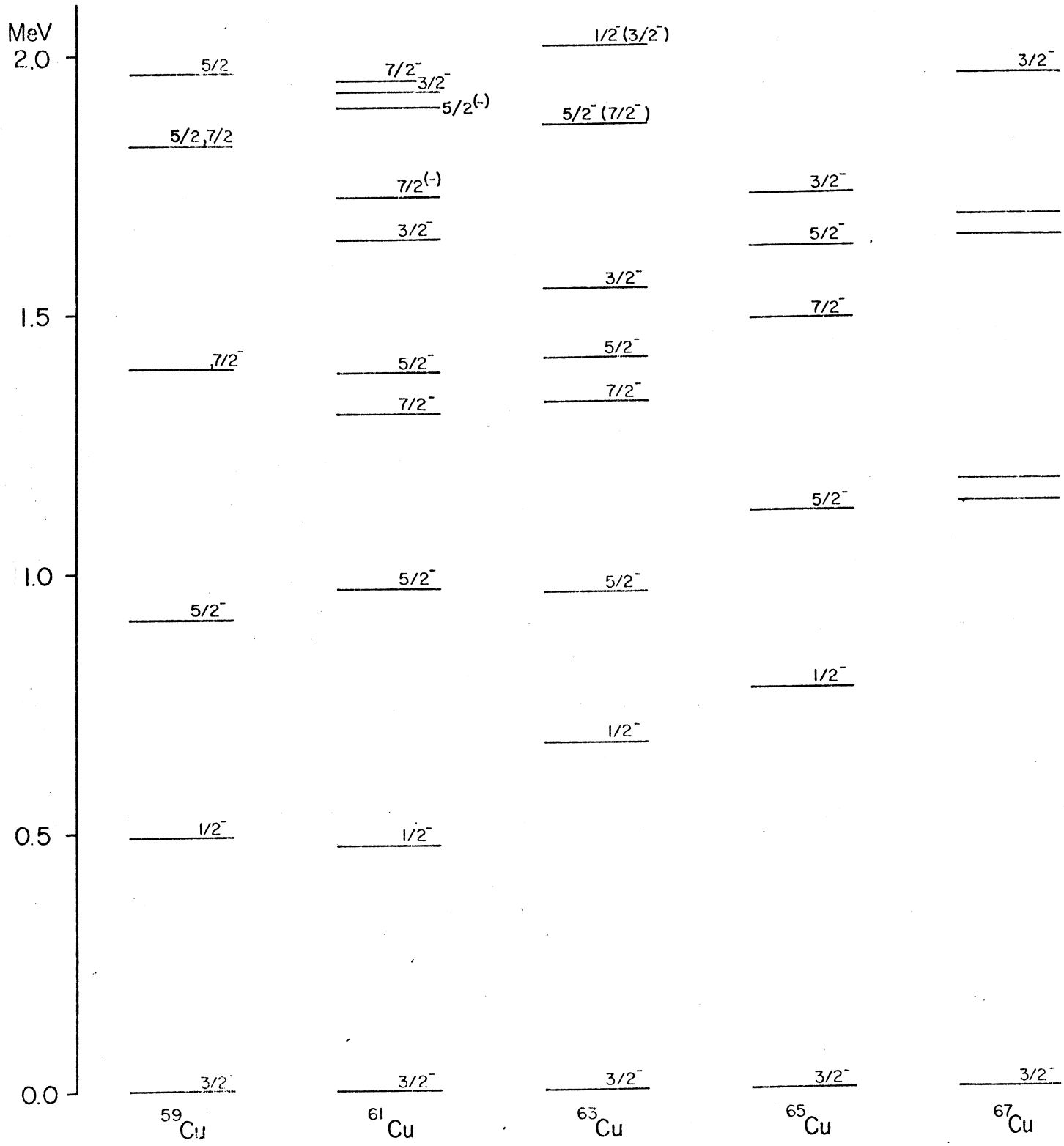
MeV
2.0
1.5
1.0
0.5
0.0
5/2
5/2,7/2
7/2⁻
5/2⁻
1/2⁻
3/2⁻
59Cu
7/2⁻
3/2⁻
5/2(-)
7/2(-)
3/2⁻
5/2⁻
7/2⁻
5/2⁻
1/2⁻
3/2⁻
61Cu
1/2⁻(3/2⁻)
5/2⁻(7/2⁻)
3/2⁻
5/2⁻
7/2⁻
5/2⁻
1/2⁻
3/2⁻
63Cu
3/2⁻
3/2⁻
5/2⁻
7/2⁻
5/2⁻
1/2⁻
3/2⁻
65Cu
3/2⁻
67Cu

Figure 8